Final Report to

European Office of Aerospace Research and Development (EOARD)
Air Force Office of Scientific Research
Air Force Research Laboratory

Project Title

Development of a robust smart antenna array signal-processing algorithm based on antenna array auto-calibration using GPS signals.

Contract No.

F73001 F30602 99MV072

Document source	Antenna Research Group, ECE, UL, Limerick / Dr. M. O'Droma
Filing	
Date	November 2002
Document ID Version No.	ARG-ARFL-PJ1.0/ VER 1.7
No. of pages	74

Antenna Research Group, ECE, UL		**ARFL**	
Approved	**Prepared**		
M.O'Droma	J. Mao A. Goacher		

Report Documentation Page

Form Approved
OMB No. 0704-0188

1. REPORT DATE	2. REPORT TYPE	3. DATES COVERED
01 OCT 2003	**N/A**	**-**

4. TITLE AND SUBTITLE	5a. CONTRACT NUMBER
Development of a robust smart antenna array signal-processing algorithmbased on antenna array auto-calibration using GPS signals.	5b. GRANT NUMBER
	5c. PROGRAM ELEMENT NUMBER
6. AUTHOR(S)	5d. PROJECT NUMBER
	5e. TASK NUMBER
	5f. WORK UNIT NUMBER
7. PERFORMING ORGANIZATION NAME(S) AND ADDRESS(ES) **University of Limerick Limerick Ireland**	8. PERFORMING ORGANIZATION REPORT NUMBER
9. SPONSORING/MONITORING AGENCY NAME(S) AND ADDRESS(ES)	10. SPONSOR/MONITOR'S ACRONYM(S)
	11. SPONSOR/MONITOR'S REPORT NUMBER(S) **SPC 01-4075**

12. DISTRIBUTION/AVAILABILITY STATEMENT
Approved for public release, distribution unlimited

13. SUPPLEMENTARY NOTES
The original document contains color images.

14. ABSTRACT

15. SUBJECT TERMS

16. SECURITY CLASSIFICATION OF:			17. LIMITATION OF ABSTRACT	18. NUMBER OF PAGES	19a. NAME OF RESPONSIBLE PERSON
a. REPORT **unclassified**	b. ABSTRACT **unclassified**	c. THIS PAGE **unclassified**	**UU**	**76**	

Table of Contents

1. History

Modified by	**Date**	**Version**	**Comments**
M. O'Droma	19 Nov.2002	1.6	Edits
M. O'Droma/J.Mao	25 Nov. 2002	1.7	Revision of some bibliographic information

2. Distribution List and Acknowledgements

2.1 Distribution List

UL

Dr. M. O Droma

Dr. J. Mao

A. Goacher

EOARD

Dr. C. Reuter

AFRL/IFGC

Dr. K. Kwiat

R. N. Smith

2.2 Acknowledgements:

University of Limerick would like to acknowledge the fulsome support for this project of European Office of Aerospace Research and Development (EOARD), Air Force Office of Scientific Research, Air Force Research Laboratory, and in particular the individual support of Drs Dan McAuliffe, John C Cleary, Barry McKinney, Kevin Kwiat, Chris Reuter and R.N. Smith.

3. Referenced Documents

Ref. No.	**Referenced Document Title**	**Document Source**
1	Contract No. **F73001 F30602 99MV072**	

4. Glossary.

BER	Bit Error Rate
BPSK	Binary Phase-Shift Keying
CDMA	Code Division Multiple Access
CRLB	Cramer-Rao Lower Bound
DGPS	Differential mode GPS
DOA	Direction of Arrival
DSP	Digital Signal Processor
ESPRIT	Estimation of Signal Parameters via Rotational Invariance Techniques
EVD	EigenValue Decomposition
GPS	Global Positioning System
GS	Gram-Schmidt (Orthoganalisation)
MCM	Mutual Coupling Matrix
ML	Maximum Likelihood
MSE	Mean Square Error
MUSIC	MUltiple SIgnal Classification
MVDR	Minimum Variance Distortionless Response
PRN	Pseudo-Random Noise
RMSE	Root Mean Square Error
SNR	Signal-to-Noise Ratio
UAV	Uninhabited Air Vehicle
UCA	Uniform Circular Array
ULA	Uniform Linear Array
WSF	Weighted Subspace Fitting

5. Introduction.

5.1 General.

For the U.S. Air Force better, more rapid decision-making is essential to achieving virtually all joint war-fighting capabilities in the 21st century battle-space. War-fighters must be assured the capability to seamlessly acquire, store, distribute and protect their information. Seamless communications span the globe; interconnecting command echelons, services, and allies worldwide by implementing common transport protocols and dynamic network management. By focusing on wide bandwidth capabilities linked to the Air Force's current narrowband tactical systems, including mitigated modems to recover messages during nuclear and naturally disturbed environments, the Air Force can provide the correct critical information to the warrior anywhere in the world. To achieve wideband seamless communications it is essential to use smart conformal wideband (2 MHz – 2 GHz) antennas. This has the added benefit of resulting in fewer antennas being required on airplanes and Uninhabited Air Vehicles (UAVs).

The University of Limerick has ongoing research in the general area of array signal processing algorithms for smart antennas. The principal general goal of this project is the development of improved robust, stable and accurate algorithms for signal source bearing estimations using sampled data taken from the sensors of phase array antennas on airplanes and UAVs. The particular goal is to investigate the feasibility of using Global Positioning System (GPS) signals to facilitate "on-the-fly" auto-calibration of phase array antennas and to develop a means of doing so.

5.2 Background.

While the potential benefits of phase array antennas are well known, with some of these having been exploited in various applications for over 50 years, the developments in DSP hardware and software are now making it feasible to exploit more and more of these benefits. This has led to a renewed interest in the field of phase array antennas and to an upsurge in the development of parameter estimation algorithms. Good bibliographies can be found in Krim & Viberg's review paper in 1996 [1] and in Dr. Tsoulos's paper [2].

A common thread running through the published literature dealing with DSP algorithm development (some of these algorithms are quite ingenious, innovative and unique) is the use of ideal array data models. This avoids consideration of the more practical problems of real dynamic array system characteristics and the resultant performance degradation. These

performance-degrading characteristics are mainly the sensor gain/phase uncertainty, the sensor location uncertainty, and the mutual coupling effect between the sensor array elements. In this project we are proposing to investigate the possibility of accounting for the real dynamic antenna array characteristics by means of an "on-the-fly" auto-calibration system using GPS signals to produce an accurate data array model. If this is achievable, and there are good reasons to believe it is, then signal parameter estimation by smart antennas could become a two-stage process:

(i) auto-calibration to yield an accurate array data model and

(ii) the signal parameter estimation itself, using this accurate array data model, with one of the more promising modern estimation algorithms (e.g. maximum likelihood or subspace methods).

There are important benefits in military applications for this technology including range extension, capacity enhancement, higher data rates, efficient management of energy resources and better BER performance. These will provide greater security of radio communication channels and more accurate target or radio source pinpointing and tracking, with more accurate control of antenna pattern nulls and peaks – an important attribute in jamming counter-measures, both effecting and resisting jamming.

With its inherent adaptive capacity to enable dynamic narrow-cast radio communications, this technology can contribute towards improvements in security, immunity to interference and robustness of communication channels whether they be used for telecommand, telecontrol, telemetry or multimedia data/voice/video exchange.

5.3 Description of Problem.

The smartness in smart antennas lies mainly in the sophisticated signal processing algorithms. These have the task of extracting the required signal parameters of multiple signal sources from the data received at the antenna array sensors. These parameters may be the number of signal sources, the signal frequencies, the directions of arrival, polarisation, etc.. This is a non-trivial multi-dimensional estimation problem, and thus the necessary signal processing algorithms are complex. The complexity of these estimation algorithms is further magnified when array model errors such as the inequality of sensor channel gain and phase characteristics, sensor location errors, and the presence of inter-sensor mutual coupling are included in the numerical model.

One way of reducing the complexity of the estimation algorithms is to characterise the array model more accurately by estimating the net effect of the various errors and using this real array model (as opposed to the ideal array model) in the parameter estimation. This requires signal sources with known parameters (frequency and location) covering the utilised array manifold. This calibration of the antenna array characteristics will lead to systems that are able to realise more reliable, robust and accurate parameter estimation. This project proposes to take an important step in this direction by attempting to develop a capability of 'on-the-fly' auto-calibration of a phase array antenna system using the known characteristics of GPS signals when operating in an otherwise unknown signal environment.

The advantage accruing from this approach is that whatever the parameters are which have to be estimated (directions of arrival, signal carrier frequencies etc.), the required smart antenna signal processing algorithms can now use an accurate array data model. Thus one significant source of doubt in the accuracy of the estimated parameters is removed. At the same time, removing the need to attempt to allow for unknown changes in the antenna physical characteristics since the 'last' calibration reduces the complexity of the estimation algorithm.

5.4 Project Objectives.

The main objective of this project was to develop an algorithm that will use the known characteristics of GPS signals, which are received by the phase array antenna, to execute 'on-the-fly' auto-calibration of the antenna array thus reducing errors due to unknown sensor channel characteristics, array characteristics and mutual coupling effects. A secondary objective was to see how such an algorithm could then be combined with an appropriate parameter estimation algorithm.

A successful outcome to this research proposal would open the possibility of designing a two-stage smart antenna signal-processing scenario for some smart antenna applications:

a) "on-the-fly" calibration of antenna array and sensor tuned receiver channels

b) estimation of the required unknown receive signal parameters.

The result should be that the accuracy and speed of parameter estimation would be much improved over that of existing approaches.

6. Global Positioning System (GPS).

6.1 Introduction.

GPS is a satellite based system which enables the positions of points on the ground or in the air to be determined with high accuracy at any time of day or night independent of weather conditions. Over the past years GPS has gone from an exciting space-age prospect to an invaluable asset in many fields such as engineering and surveying as well as all aspects of navigation. Currently GPS comprises a constellation of 24 satellites. There are 4 satellites in each of 6 equispaced orbits that have an inclination of 55º - see Fig 6.1.

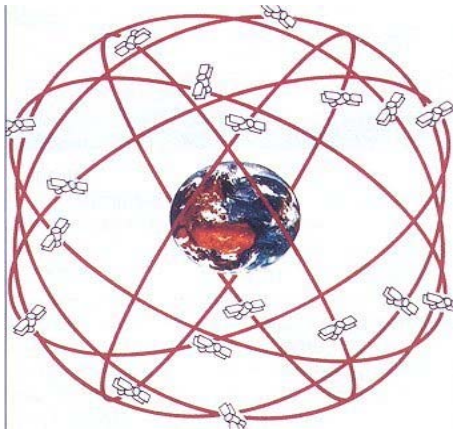

Fig 6.1 Global Positioning System (GPS) Constellation.

GPS uses the principle of triangulation to calculate a user receiver's position relative to a set of known points. These known points are the positions of the satellites (see Fig 6.2) as they orbit the earth and broadcast their positions and a consistent time standard called GPS System Time. The receiver uses the location of each satellite, the system time, its clock biased relative to GPS system time and the time of arrival of the signal to compute its distance from each satellite. More sophisticated user equipment also uses Doppler readings to aid in computing the receiver velocity or to provide highly accurate navigation solutions.

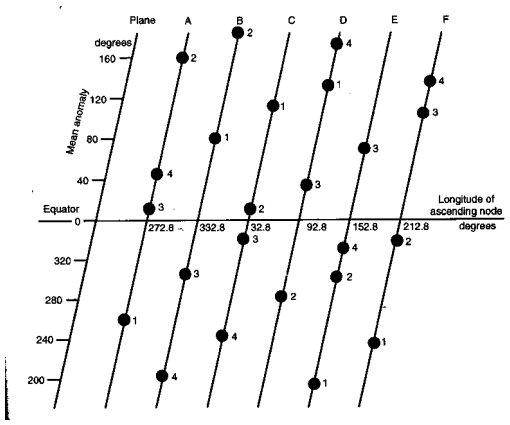

Fig 6.2 GPS Constellation – planar projection.

6.2 GPS Features.

The theory behind GPS can be quite easily understood without going into the complex mathematics of the system. The distance (range) between any satellite and receiver can be calculated by measuring the time taken by a radio signal to travel from the satellite to the receiver. The geometry of the system is such that if three ranges are measured simultaneously then the user can calculate his position using a computational technique known as resection. However, in order to solve all of the mathematical unknowns four satellite ranges are generally required. These satellites must be visible to the receiver and also scattered across the sky in such a way as to provide a good geometric arrangement with respect to the receiver. As each satellite transmits mutually exclusive signals it is possible to distinguish between information received from different satellites. Current GPS receivers can accept information from up to 8 different satellites simultaneously. The type of information extracted from the signal and the obtainable accuracy depends on the type of receiver used.

There are two categories of receiver - those capable of reading the code signal only and those capable of reading both the code and the carrier phase signals simultaneously. Both types of receiver support two unique codes - the C/A (Coarse Acquisition) -code and the P (Precise) -code. The C/A-code is not very complex, is easy for a receiver to lock on to and is available to all civilian users. The P-code, on the other hand, although more difficult to acquire, is more accurate. Code only receivers can be used in one of two modes and the accuracy achieved depends on the method of use. In a stand-alone mode only one receiver is

necessary in order to compute an approximate position by resection. The positional accuracy is generally good to ±20m, but it is only reliable to ±100m. The American military, who control the GPS satellites, have the ability to downgrade the satellite signal through a process known as Selective Availability (SA) and it is this that limits the accuracy of code only receivers. Although SA degrades the determination of absolute positioning, it has little effect on the relative position between two close receivers as the error in the received signals will be similar in both receivers and thus cancel out. Accuracies of ±1m can be obtained by using two or more code-only receivers operating simultaneously; this is known as differential mode GPS (DGPS). In this mode of operation the resection solutions at each ground station can be related to each other producing accurate co-ordinate differences between the two stations rather than absolute positions.

Since metre level accuracy is inadequate for most surveying or engineering jobs a second category of receivers, known as code and carrier phase receivers, must be used to achieve the required accuracy. These receivers are only designed for use in differential mode. They record both the C/A-code and the P-code (when available) and also use the carrier phase as a means of fine interpolation. Each satellite transmits two carrier frequencies, L1 and L2, and consequently there are two types of code and phase receiver available - single frequency, which use the information available on L1 only, and dual frequency, which use both frequencies.

6.3 GPS Signal Characteristics.

GPS satellite transmissions utilise direct sequence, spread spectrum (DSSS) modulation. DSSS provides the structure for the transmission of ranging signals and essential navigation data such as satellite ephemeredes and satellite height. The ranging signals are pseudo-random noise (PRN) codes that binary phase shift key (BPSK) modulate the satellite carrier frequencies. These codes look like and have spectral properties similar to random binary sequences, but are actually deterministic. They have a predictable pattern that is periodic and can be replicated by a suitably equipped receiver. Each GPS satellite broadcasts two PRN ranging codes; a ‘short’ C/A-code and a ‘long’ P-code. The C/A-code has a period of 1 msec and repeats constantly, whereas the P-code is a seven-day sequence that repeats every Saturday/Sunday midnight. At the time of writing the P-code is encrypted and is known as the Y-code. This Y-code is only accessible to selected users through the use of cryptography.

The GPS satellites transmit on two carrier frequencies called L1, the primary frequency, and L2, the secondary frequency. Each carrier frequency is modulated by the navigation data message and then the spectrum spread by modulation with a PRN sequence unique to the satellite. All satellites transmit on the same two carrier frequencies, but their signals to not interfere significantly because each has a unique PRN code and the PRN codes are selected to be, as far as possible, uncorrelated with each other. Because the PRN codes are nearly uncorrelated, the signals from each satellite can be detected and separated using code division multiple access (CDMA). In order to track one satellite in common view with several others using the CDMA technique, the receiver must replicate the PRN sequence for the desired satellite along with the replica carrier signal, including Doppler effects.

Two carrier frequencies are transmitted to enable two-frequency users to measure the ionospheric delay. This delay effects the accuracy of the time measurement and can be measured using two frequencies since this delay is related by a scale factor to the difference in signal time-of-arrival for the two carrier frequencies. Single-frequency (L1 only) users must estimate the ionospheric delay using modeling parameters that are broadcast to the user in the navigation message.

6.4 Using GPS to Calibrate Antenna Arrays.

GPS is a system that enables a user to calculate his position from the times-of-arrival of the signals from a number of satellites. It is a simple step, knowing the location of the user and the positions of the various satellites in space, to calculate the directions-of-arrival (DOAs) of the satellite signals. It is the knowledge of these DOAs, in azimuth and elevation with respect to the reference plane of the antenna array, that will enable the calibration of the antenna array and thus reduce errors due to unknowns such as physical distortions and mutual coupling effects. Fig. 6.3 shows how four GPS satellites could be used as calibration sources with known azimuth and elevation.

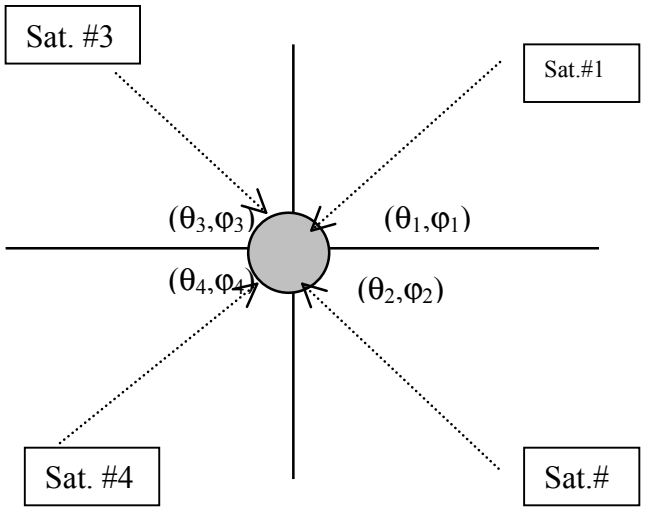

Fig. 6.3 GPS Signals as Calibration Sources

7. Antenna Array Model.

7.1 Modelling the Antenna Array.

Consider an antenna array composed of M antenna sensors arbitrarily located in space and assume that a signal s(t) impinges on the array. Let τ_m be the propagation time delay of the signal at the m^{th} sensor, related to a fixed point. Assuming that the antenna can be modelled as a linear system and letting $h_m(t)$ be the impulse response of the m^{th} sensor, then the output of the m^{th} sensor can be written as:

$$x_m(t) = h_m(t) \alpha s(t - \tau_m) + n_m(t)$$

where αdenotes convolution and $n_m(t)$ is the additive noise, which is independent of the signal.

Let signal s(t) be a modulated signal with carrier angular frequency ω_c (= $2\pi f_c$) and modulation amplitude a(t) and phase $\phi(t)$ such that:

$$s(t) = a(t) \cos(\omega_c t + \phi(t))$$

If the signal being considered is narrowband, i.e. the envelope variations, amplitude a(t) and phase $\phi(t)$, of the signal vary slowly relative to the propagation time across the array, then:

$$a(t - \tau_m) \cong a(t), \qquad \phi(t - \tau_m) \cong \phi(t)$$

Hence, we may write the received signal s(t) as:

$$s(t- \tau_m) = a(t - \tau_m) \cos(\omega_c(t - \tau_m) + \phi(t - \tau_m))$$

$$\cong a(t) \cos(\omega_c(t - \tau_m) + \phi(t))$$

and the output of the m^{th} sensor may be written as:

$$x_m(t) = h_m(t) \alpha s(t - \tau_m) + n_m(t)$$

$$\cong h_m(t) \alpha a(t) \cos(\omega_c(t - \tau_m) + \phi(t)) + n_m(t)$$

The narrowband assumption is most often satisfied when the signal bandwidth is much smaller than the carrier frequency and the signal propagation time across the array is smaller than the inverse of the array aperture. This assumption can also be satisfied for wideband signals, such as in the case of CDMA, if the frequency response of each antenna sensor is approximately flat over the signal bandwidth. Using this narrowband assumption, the propagation time delay across the array can be modelled as a simple phase shift and the signals have bandpass characteristics about the centre frequency. The complex representation of the output of the m^{th} sensor can then be given as:

$$X_m(t) = H_m(\omega_c) \exp(-j\omega_c\tau_m) s(t) + n_m(t)$$

where $H_m(\omega_c)$ is the frequency response of the m^{th} sensor (i.e. the Fourier transform of $h_m(t)$).

Given the assumption that each antenna sensor can be modelled as a linear element, the resultant sensor output signal is a superposition of the p individual signals received. Here, we introduce the parameter vector $\boldsymbol{\eta}_n$ (n = 1,2,…,p) to denote the collection of parameters, such as bearing, elevation, frequency, polarisation and so on, associated with the n^{th} signal. The impulse response and time delay of each sensor can be represented as a function of the parameter vector $\boldsymbol{\eta}_n$ so that the data model for the m^{th} sensor output can be rewritten as:

$$X_m(t) = \sum_{i=1}^{p} H_m(\boldsymbol{\eta}_i)\exp(-j\omega_c\tau_m(\boldsymbol{\eta}_i))s_i(t) + n_m(t) = \sum_{i=1}^{p} a_m(\boldsymbol{\eta}_i)s_i(t) + n_m(t)$$

Since the array comprises M sensors, the output vector for the array is given by:

$$\begin{aligned}\mathbf{X}(t) &= \begin{pmatrix} X_1(t) \\ \vdots \\ X_M(t) \end{pmatrix} = \sum_{i=1}^{p} \begin{pmatrix} a_1(\boldsymbol{\eta}_i) \\ \vdots \\ a_M(\boldsymbol{\eta}_i) \end{pmatrix} s_i(t) + \begin{pmatrix} n_1(t) \\ \vdots \\ n_M(t) \end{pmatrix} \\ &= \sum_{i=1}^{p} \mathbf{a}(\boldsymbol{\eta}_i)s_i(t) + \mathbf{n}(t) \\ &= [a(\boldsymbol{\eta}_1),\cdots,a(\boldsymbol{\eta}_p)] \begin{pmatrix} s_1(t) \\ \vdots \\ s_p(t) \end{pmatrix} + \mathbf{n}(t) \\ &= \mathbf{A}(\boldsymbol{\eta})\mathbf{S}(t) + \mathbf{n}(t)\end{aligned}$$

where the vector $\mathbf{a}(\boldsymbol{\eta})$ is referred to as the array response vector or steering vector and is given by :

$$\mathbf{a}(\boldsymbol{\eta}) = [H_1(\boldsymbol{\eta})\exp(-j\omega_c\tau_1(\boldsymbol{\eta})) \quad H_2(\boldsymbol{\eta})\exp(-j\omega_c\tau_2(\boldsymbol{\eta})) \quad \cdots \quad H_M(\boldsymbol{\eta})\exp(-j\omega_c\tau_M(\boldsymbol{\eta}))]^T$$

and $a(\boldsymbol{\eta})$ is a function of the parameter vector $\boldsymbol{\eta}$, $\boldsymbol{\eta} = [\boldsymbol{\eta}_1^T, \ldots, \boldsymbol{\eta}_p^T]^T$.

If there are N (<M) elements (different parameters) in $\mathbf{a}(\boldsymbol{\eta})$, then $\boldsymbol{\eta}$ will trace an N-dimensional surface in C^M as $\boldsymbol{\eta}$ is varied over the parameter space. This surface is referred to as the array manifold and is denoted:

$$\mathbf{A} = \{\mathbf{a}(\boldsymbol{\eta}) : \boldsymbol{\eta} \in \boldsymbol{\theta}\}$$

where $\boldsymbol{\theta}$ denotes the set of all possible parameter vectors of interest.

The noise process, $\mathbf{n}(t)$, is assumed to be a zero-mean, stationary random process and the probability of distribution of the noise is assumed to be circular complex Gaussian, i.e. the real and imaginary parts of $\mathbf{n}(t)$ are independent, and with the second order moments:

$$E\{\mathbf{n}(t)\mathbf{n}^H(\tau)\} = \mathbf{Q}\,\delta(t,\tau)$$

$$E\{\mathbf{n}(t)\mathbf{n}^T(\tau)\} = 0$$

where E{.} and δ represent the statistical expectation and Kronecker delta function respectively. In this analysis, the background noise is assumed to be spatially white so that the noise covariance matrix, **Q**, is a scaled identity matrix $\sigma^2\mathbf{I}$, where σ^2 is the noise variance.

In this paper, since we are considering signals of known frequency, we are only interested in the parameters of signal azimuth and elevation. The array manifold can, therefore, be described as:

$$\mathbf{A} = \{\mathbf{a}(\theta,\phi) : \theta,\phi \in \mathbf{\Theta}\}$$

which is a two-dimensional surface in space C^M, where θ and ϕ denote the signal azimuth and elevation respectively.

Thus, the output vector for the array can be rewritten as:

$$\begin{aligned} X(t) &= \sum_{i=1}^{p} a(\theta_i,\phi_i)s_i(t) + \mathbf{n}(t) \\ &= \mathbf{A}(\boldsymbol{\theta},\boldsymbol{\varphi})\mathbf{S}(t) + \mathbf{n}(t) \end{aligned}$$

where the steering vector:

$$\mathbf{a}(\theta_i,\phi_i) = \left[H_1(\theta_i,\phi_i)e^{-j\omega_c\tau_1(\theta_i,\phi_i)} \quad H_2(\theta_i,\phi_i)e^{-j\omega_c\tau_2(\theta_i,\phi_i)} \quad \cdots \quad H_M(\theta_i,\phi_i)e^{-j\omega_c\tau_M(\theta_i,\phi_i)}\right]^T$$

If we assume each array sensor has the same response, then $H_1(\theta_n,\phi_n) = H_M(\theta_n,\phi_n) = H(\theta_n,\phi_n)$. Thus, $\mathbf{a}(\theta_i,\phi_i)$ is a function of τ_m only and can be written:

$$\mathbf{a}(\theta_i,\phi_i) = H(\theta_i,\phi_i)\left[e^{-j\omega_c\tau_1(\theta_i,\phi_i)} \quad e^{-j\omega_c\tau_2(\theta_i,\phi_i)} \quad \cdots \quad e^{-j\omega_c\tau_M(\theta_i,\phi_i)}\right]^T$$

In the ideal case, the time delay at each element can be calculated for any θ and ϕ from the array geometry and the signal frequency, and the calibration of the array depends only on determining the sensor response H(θ,ϕ).

7.2 Modelling Systemic Errors.

Whilst, in the ideal case, the steering vector can be calculated from knowledge of the array geometry, in practice there are a number of sources of error in any system. These may be grouped under two headings.

Firstly, there are errors in amplitude and phase in the tracking between the different sensors and their associated circuitry. These may be due to inherent imbalances between the sensors and their associated circuitry (amplifiers, cables, digitisers, etc.) or they may be changes in any part of the system due to temperature or aging effects.

Consider p radiating sources observed by an array of M antenna sensors. The signal output of the m^{th} sensor can be described by:

$$x_m(t) = \sum_{n=1}^{p} \alpha_m s_n(t - \tau_{mn} - \psi_m) + n_m(t)$$

where $s_n(t)$ (n = 1, 2, …p) represents the received signals, α_m and ψ_m are the gain and phase delay associated with the m^{th} sensor and its circuitry and τ_{mn} is the delay relative to a reference point associated with the signal propagation from the n^{th} source to the m^{th} sensor.

In matrix notation the array output can be expressed as:

$$\mathbf{X}(t) = \mathbf{\Gamma A}(\boldsymbol{\theta}, \boldsymbol{\varphi})\mathbf{S}(t) + \mathbf{N}(t)$$

where -

$\mathbf{X}(t) = [x_1(t) \quad x_2(t) \quad \cdots \quad x_M(t)]^T$

$\mathbf{S}(t) = [s_1(t) \quad s_2(t) \quad \cdots \quad s_M(t)]^T$

$\mathbf{N}(t) = [n_1(t) \quad n_2(t) \quad \cdots \quad n_M(t)]^T$

$\mathbf{\Gamma} = \text{diag}[\alpha_1 e^{j\omega_c \psi_1} \quad \alpha_2 e^{j\omega_c \psi_2} \quad \cdots \quad \alpha_M e^{j\omega_c \psi_M}]^T$ contains the amplitude and phase errors

$\mathbf{A}(\boldsymbol{\theta}, \boldsymbol{\varphi}) = [\mathbf{a}(\theta_1, \phi_1) \quad \mathbf{a}(\theta_2, \phi_2) \quad \cdots \quad \mathbf{a}(\theta_N, \phi_N)]$

Secondly, there are mutual coupling effects between the antenna sensors that make up the array. When antenna sensors are in close proximity, typically less than half a wavelength, the impedance and polar response of each sensor is affected by the electromagnetic coupling to its adjacent sensors. This will distort the radiation pattern of the array and hence modify the array manifold. The output of the m^{th} sensor, in the absence of other sources of error, may now be written as:

$$x_m(t) = \sum_{i=1}^{M} C_{m,i} \mathbf{a}_i(\theta, \phi)\mathbf{S}(t) + \mathbf{N}(t)$$

where $C_{m,i}$ (i, m = 1, 2, …M) is the mutual coupling factor and models the mutual coupling effect of the i^{th} sensor on the m^{th} sensor and $\mathbf{a}_i(\theta,\phi)$ is the i^{th} row of the steering matrix $\mathbf{A}(\theta,\phi)$.

Thus, the output of the array is given by:

$$\mathbf{X}(t) = \mathbf{C}\ \mathbf{A}(\theta,\phi)\ \mathbf{S}(t) + \mathbf{N}(t)$$

where **C** is an M x M complex matrix taking account of all effects due to mutual coupling between sensors and is referred to as the Mutual Coupling Matrix. In general, the matrix **C** has no special structure; however, if the array is uniform, then the matrix will be structured because coupling between adjacent sensors is common to sensors occupying a similar position in the array and coupling between non-adjacent sensors may be ignored.

When both types of error are considered the array output may be written as:

$$\mathbf{X}(t) = \mathbf{\Gamma}\ \mathbf{C}\ \mathbf{A}(\theta,\phi)\ \mathbf{S}(t) + \mathbf{N}(t)$$

$$= \mathbf{A'}(\theta,\phi)\ \mathbf{S}(t) + \mathbf{N}(t)$$

where **A'** represents the actual steering matrix, allowing for all sources of error, at frequency f_c. It is this matrix that will be calculated from GPS measurements and provide a calibration of the antenna array.

8. Parameter Estimation Methods.

8.1 Introduction.

As shown in section 7.1, the output vector for a perfect array (i.e. ignoring amplitude or phase imbalances and the effects of mutual coupling between array sensors) can be given by:

$$\mathbf{X}(t) = \mathbf{A}(\theta,\phi)\,\mathbf{S}(t) + \mathbf{N}(t)$$

where the array manifold $\mathbf{A}(\theta,\phi)$ can be calculated from the array geometry and the operating frequency.

This means that, assuming the array manifold is unambiguous, it is possible, by suitable processing of the received signal, to calculate the azimuth and elevation of the signal. This involves using spatial processing technology to generate a spatial data matrix from which the desired parameters can be estimated by using an appropriate algorithm.

In this section we will review some of the main estimation methods; beamforming, subspace-based methods and maximum likelihood methods.

8.2 Beamforming Techniques.

Digital beamforming is a product of merging antenna technology and digital signal processing technology. Early applications of digital beamforming were developed for sonar and radar systems. One of their major advantages is that all of the desired information being carried by the signals may be extracted in the form of digital streams and made available for processing in the beamformer. Using this information and suitable algorithms, the beamformer can be driven to produce different types of beams such as scanning beams, multiple beams, shaped beams or beams with steered nulls. There are many different configurations that may be used to achieve these beamformins and Fig. 8.1 depicts a typical beamformer structure. The beamformer forms a linear combination of the antenna outputs, first multiplying each output by a complex weight and then summing them together.

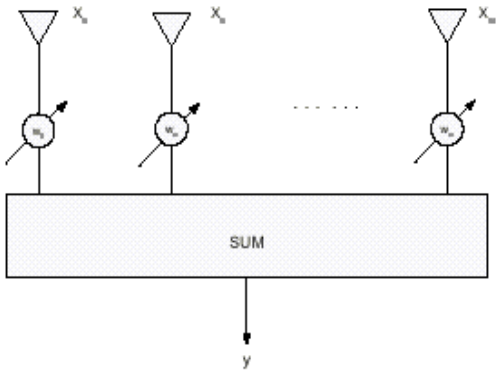

Fig. 8.1 A typical beamformer structure.

8.2.1 Coventional Beamformer.

The conventional beamformer is a natural extension of classical Fourier-based spectral analysis [3] to array data. The beamformer maximizes the power of the array output for a given input signal:

$$\mathbf{x}(t) = \mathbf{a}(\theta,\phi)s(t) + \mathbf{n}(t)$$

If we want to maximize the output power from a specific direction (θ,ϕ) then, for the conventional beamformer, the output of the beamformer at time t, y(t), is given by a linear combination of the data at M antenna sensors at time t:

$$y(t) = \sum_{m=1}^{M} w_m^H x_m(t)$$

where $x_m(t)$ is the signal from the m^{th} antenna sensor of the array and w_m is the weight applied to $x_m(t)$. In vector form, this can be written as:

$$\mathbf{y}(t) = \mathbf{w}^H\mathbf{x}(t)$$

Hence, the problem of maximizing the output power is formulated as:

$$\begin{aligned}\arg\max_w P(\mathbf{w}) &= \arg\max_w E\{\mathbf{w}^H\mathbf{x}(t)\mathbf{x}^H(t)\mathbf{w}\}\\ &= \arg\max_w \mathbf{w}^H E\{\mathbf{x}(t)\mathbf{x}^H(t)\}\mathbf{w}\\ &= \arg\max_w \{E|s(t)|^2|\mathbf{w}^H\mathbf{a}(\theta,\phi)|^2 + \sigma^2|\mathbf{w}|^2\}\end{aligned}$$

Here we assume the noise is spatially white and the norm of **w** is constrained to $|\mathbf{w}|=1$. Then, the resulting solution is:

$$\mathbf{w}_{BF} = \frac{\mathbf{a}(\theta,\phi)}{\sqrt{\mathbf{a}^H(\theta,\phi)\mathbf{a}(\theta,\phi)}}$$

and the classic beamforming spatial spectrum is given by:

$$P_{BF} = \frac{\mathbf{a}^H(\theta,\phi)\hat{\mathbf{R}}\mathbf{a}(\theta,\phi)}{\mathbf{a}^H(\theta,\phi)\mathbf{a}(\theta,\phi)}$$

where $\hat{\mathbf{R}}$ is the estimation of the sample covariance matrix.

8.2.2 Constrained Beamformer (Capon Beamformer).

The conventional beamformer has the limitation that it cannot resolve two sources spaced closer than the beamwidth of the array. Modifications to improve this limitation have been proposed by many researchers. One of the best known is the constrained (or minimum variance distortionless response –MVDR) beamformer proposed by Capon [4]. The optimization problem for the output power is:

$$\arg\min_{w} P(\mathbf{w}) = \arg\min_{w} E\left\{\left|\mathbf{w}^H\mathbf{x}(t)\right|^2\right\}$$

$$\text{such that : } \mathbf{w}^H\mathbf{a}(\theta,\phi) = 1$$

The optimal **w** can be obtained by using the Lagrange multiplier technique:

$$\mathbf{w}_{MVDR} = \frac{\hat{\mathbf{R}}^{-1}\mathbf{a}(\theta,\phi)}{\mathbf{a}^H(\theta,\phi)\hat{\mathbf{R}}^{-1}\mathbf{a}(\theta,\phi)}$$

and the Capon (MVDR) beamformer beam pattern is given by:

$$P_{MVDR}(\theta,\phi) = \frac{1}{\mathbf{a}^H(\theta,\phi)\hat{\mathbf{R}}^{-1}\mathbf{a}(\theta,\phi)}$$

8.3 Subspace DOA Estimation Methods

Subspace, or eigen-structure, methods were developed from the spectral decomposition of the covariance matrix, the so-called Pisarenko's harmonic decomposition method, and were first introduced via the MUSIC algorithm [5]. Many subspace, or eigen-structure, methods are proposed in the literature due to its high-resolution property [6] [7] and the MUSIC algorithm has been received more attention.

8.3.1 Subspace Properties.

If d signals impinge on an antenna array comprising M sensors, then the array output covariance matrix,

$$\mathbf{R}_{xx} = E\left\{\mathbf{X}\mathbf{X}^H\right\} = \mathbf{A}(\theta,\phi)\mathbf{P}\mathbf{A}^H(\theta,\phi) + \sigma^2\mathbf{I}$$

where $\mathbf{A}(\theta,\phi)$ is the $M \times d$ steering matrix, **P** is the $d \times d$ signal covariance matrix.

Let d' denote the rank of signal covariance matrix **P**. Then, if $d' < d$ some of the signals are coherent, (i.e., one signal is a copy of another with a complex constant, such as multipath

signals) and the signal covariance matrix **P** will not be full rank, d, but rather with rank d'. Let the eigen-decomposition of R_{xx} be:

$$R_{xx} = \sum_{k=1}^{M} \lambda_k e_k e_k^*$$

where the eigenvalues are ordered as $\lambda_1 \geq \lambda_2 \geq \ldots \geq \lambda_M$ and are orthogonal and $e^*_k e_l = \delta(k,l)$ due to the $\mathbf{R}_{xx}$ being Hermitean. The rank of $\mathbf{A}(\theta,\phi)\mathbf{P}\,\mathbf{A}(\theta,\phi)$ is d', and its null space has M-d' eigenvalues equal to σ^2 with the remainder d' eigenvalues larger than noise variance. Then, $\mathbf{R}_{xx}$ can be partitioned as:

$$\mathbf{R}_{xx} = \mathbf{E}_s \mathbf{\Lambda}_s \mathbf{E}_s^* + \sigma^2 \mathbf{E}_n \mathbf{E}_n^*$$

where $\mathbf{\Lambda}_s = \mathrm{diag}(\lambda_1, \lambda_2, \ldots, \lambda_{d'})$ and the corresponding space spanned by $\mathbf{E}_s$ is called the signal subspace and $\mathbf{E}_n$ is the noise subspace.

Subspace methods are based on the following observations:

$$R(\mathbf{E}_s) \subseteq R(\mathbf{A}(\theta,\phi)) \quad \text{and} \quad \mathbf{E}_s \perp \mathbf{E}_n$$

where $R(\cdot)$ denotes the range of space and $\perp$ denotes " orthogonal to".

8.3.2 MUSIC (Multiple SIgnal Classification)

MUSIC (Multiple SIgnal Classification) was one of the first subspace methods to be introduced to the DOA estimation problem. In the MUSIC method, it is assumed that the signal covariance matrix, **P**, is full rank, which means d' = d and that there are no coherent signals coming to the array. Due to $R(\mathbf{E}_s) \subseteq R(\mathbf{A}(\theta,\phi))$ and $\mathbf{E}_s \perp \mathbf{E}_n$, we have

$$\mathbf{a}^*(\theta_k,\phi_k)\,\mathbf{E}_n = 0 \qquad k=1, \ldots, d$$

and the noise space **E**n is obtained by choosing the eigenvectors corresponding to the (m-d) smallest eigenvalues of $\mathbf{R}_{xx}$. The MUSIC "spatial spectrum" is then defined as:

$$P_{\mathrm{MUSIC}}(\theta,\phi) = \frac{\mathbf{a}^H(\theta,\phi)\mathbf{a}(\theta,\phi)}{\mathbf{a}^H(\theta,\phi)\hat{\mathbf{E}}_n\hat{\mathbf{E}}_n^H\mathbf{a}(\theta,\phi)}$$

The MUSIC estimates of the DOAs are obtained from the d largest peaks in the spatial spectrum with searching in space $\{\theta,\phi\}$. When d'< d, (i.e., there are coherent signals) the true steering vectors are not orthogonal to the noise subspace. The MUSIC algorithm cannot handle this scenario and will not provide correct DOAs.

8.3.3 ESPRIT (Estimation of Signals Parameters via Rotation Invariance Techniques)

ESPRIT (Estimation of Signal Parameters via Rotational Invariance Techniques) [7] is a computationally efficient and robust method of DOA estimation. This method is based on a particular type of array geometry, which uses two identical arrays, see Fig. 8.2, to form

matched pairs with an identical displacement vector, i.e., the second element of each pair ought to be displaced by the same distance and direction relative to the first element. If each subarray has M sensors it is not necessary for the whole array to have 2M sensors as sensors may be common between the two subarrays. If two elements are separated by a displacement d_0 and the signals induced on the i^{th} pair are denoted by $x_i(t)$ and $y_i(t)$, then we have:

$$y_i(t) = x_i(t)e^{j\mu_i}$$

where $\mu_I = 2\pi d_0 \xi_i/\lambda_c$ and $\xi_i = \sin\theta_i e^{-j\phi i}$, a measure of the DOA of the signal, and:

$$\mathbf{x}(t) = \mathbf{A}(\theta,\phi)\mathbf{s}(t) + \mathbf{n}_x(t)$$
$$\mathbf{y}(t) = \mathbf{A}(\theta,\phi)\mathbf{\Phi}\mathbf{s}(t) + \mathbf{n}_y(t)$$

where $\mathbf{\Phi}$ is an M×M diagonal matrix, with its m^{th} diagonal element given by:

$$\Phi_{mm} = e^{j\mu_m}$$

and $\mathbf{A}(\theta,\phi)$ is the M × N steering matrix (with N steering vectors corresponding to the N directional sources), $\mathbf{s}(t)$ denotes the N source signals induced on a reference antenna element, and $\mathbf{n}_x(t)$ and $\mathbf{n}_y(t)$ denote the noise induced on the elements of two subarrays.

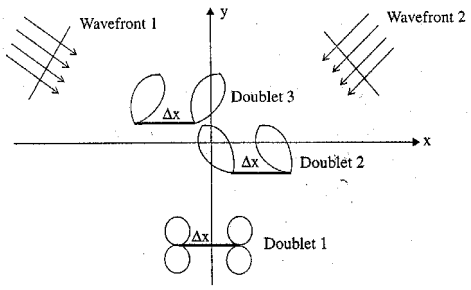

Fig. 8.2 Illustration of ESPRIT array geometry

With eigen-decomposition applied to the correlation matrices R_{xx} and R_{yy}, two M×N matrices, E_{xs} and $E_{ys,}$ with their columns denoting the N eigenvectors corresponding to the largest eigenvalues in the matrices R_{xx} and R_{yy}, are obtained. They span the same N-dimensional signal subspace and are related by:

$$\mathbf{E}_{ys} = \mathbf{\Psi}\mathbf{E}_{xs}$$

where $\mathbf{\Psi}$ is a unique nonsingular transformation matrix. Similarly, matrices $\mathbf{A}(\theta,\phi)$ and $\mathbf{A}(\theta,\phi)\mathbf{\Phi}$ are related by another unique nonsingular matrix $\mathbf{T}$, as the same signal subspace is spanned by these steering vectors. So,

$$\mathbf{E}_{xs} = \mathbf{A}(\theta,\phi)\mathbf{T} \quad \text{and} \quad \mathbf{E}_{ys} = \mathbf{A}(\theta,\phi)\mathbf{\Phi}\mathbf{T}$$

If the signal steering matrix has full rank, i.e., rank$\{\mathbf{A}(\theta,\phi)\}$=N, we have:

$$\mathbf{T}\Psi\mathbf{T}^{-1} = \Phi$$

which implies that the eigenvalues of Ψ are equal to the diagonal element of the Φ matrix and that the columns of $\mathbf{T}$ are eigenvectors of Ψ. An eigen-decompostion of Ψ gives its eigenvalues, and equating them to Φ leads to a DOA estimation. If λ_n is an eigenvalue of Ψ, then:

$$\xi_n = \sin^{-1}\left\{\frac{\mathrm{Arg}(\lambda_n)}{2\pi d_0}\right\}, \qquad n = 1,2,\cdots,N$$

8.3.4 WSF (Weighted Subspace Fitting)

The Weighted Subspace Fitting (WSF) approach [6] is a Maximum Likelihood (ML) - like algorithm based on subspace decomposition which does not use the orthogonality between

$$\min_{\theta,\phi,\mathbf{T}} \left\| \hat{\mathbf{E}}_s - \mathbf{A}(\theta,\phi)\mathbf{T} \right\|_{\mathbf{W}}^2$$

the noise subspace and the steering vector directly. Instead, it tries to fit an estimate of the signal subspace to the parameters that are of interest using a ML-like minimization. Due to $R(\mathbf{E}_s) \subseteq R(\mathbf{A}(\theta))$, the WSF approach relies on the following criterion, which gives the best weighed least squares fit of the subspaces $\mathbf{E}_s$ and $\mathbf{A}(\theta,\phi)$:

where $\|\mathbf{A}\|^2_w$ denotes *Trace*$\{\mathbf{AWA}^*\}$, and $\mathbf{T}$ is an arbitrary (d×d') matrix. The weighting $\mathbf{W}$ is a (d×d') Hermitean positive definite matrix. It is possible to explicitly solve the above equation with respect to $\mathbf{T}$ and the solution is given by:

$$\hat{\mathbf{T}} = (\mathbf{A}^*\mathbf{A})^{-1}\mathbf{A}^*\mathbf{E}_s = \mathbf{A}^+\mathbf{E}_s$$

and

$$V(\theta,\phi) = \left\| \hat{\mathbf{E}}_s - \mathbf{A}\mathbf{A}^+\mathbf{E}_s \right\|_{\mathbf{W}}^2 = \left\| \Pi_A^{\perp} \hat{\mathbf{E}}_s \right\|_{W}^2 = \mathrm{Tr}\{\Pi_A^{\perp}\mathbf{E}_s\mathbf{W}\mathbf{E}_s^*\}$$

where $\Pi_A^{\perp} = \mathbf{I} - \Pi_A = \mathbf{I} - \mathbf{A}\mathbf{A}^+$ is the orthogonal projector onto the null-space of $\mathbf{A}^H$.

The estimate of (θ,ϕ) is obtained as the minimizing argument of $V(\theta,\phi)$, i.e:

$$(\hat{\theta},\hat{\phi}) = \arg\min_{\theta,\phi} V(\theta,\phi)$$

Different choices of the weighing matrix $\mathbf{W}$ lead to a whole class of estimates. The optimal weighting matrix $\mathbf{W}_{opt}$ can be given by

$$\mathbf{W}_{opt} = (\Lambda_s - \sigma^2\mathbf{I})^2\Lambda_s^{-1}$$

The unknown quantities, $\mathbf{\Lambda}_s$ and σ^2, can be replaced by their estimation, $\hat{\mathbf{\Lambda}}_s$ and $\hat{\sigma}^2$ respectively, without effecting the asymptotic properties of estimate.

8.4 Maximum Likelihood Estimation Method (MLEM)

The Maximum Likelihood Estimation Method (MLEM) was introduced by Fisher [8] as a general estimator in statistics and has now become a powerful estimator in the signal processing area. ML estimates have strong statistical properties and the ML estimator can attain the Cramer-Rao Lower Bound (CRLB) asymptotically with the number of samples. The CRLB is a lower bound on the estimation error variance for any unbiased estimator.

From the array data model we made before, the array response data, **X**(t), given J samples, becomes a stationary, zero-mean, complex Gaussian process with unknown parameters (θ,ϕ), the direction of arrival of the signal, and **P** the signal covariance matrix. The probability density function is given by:

$$p(\mathbf{X}(1),\cdots,\mathbf{X}(J)/(\theta,\phi),\mathbf{S}(t),\sigma^2) = \prod_{t=1}^{J} \pi\sigma^2 \quad^{-M} \exp(-\frac{1}{\sigma^2}\left\|\mathbf{X}(t)-\mathbf{A}\mathbf{S}(t)\right\|^2)$$

where (θ,ϕ) is the directional information, **S**(t) is the transmitted signal and σ^2 is the variance of the noise process. The ML estimates of these unknowns are calculated as the maximising arguments of p(**X**(t)/ (θ,ϕ)**,S**(t)**,** σ^2), the rationale being that these values make the probability of the observations as large as possible. Alternatively, it is possible to minimize the negative log-likelihood function that is given by:

$$-\ln(p(\mathbf{X}(t)/(\theta,\phi),\mathbf{S}(t),\sigma^2)) = M\ln\sigma^2 + \frac{1}{\sigma^2 J}\sum_{t=1}^{J}\left\|\mathbf{X}(t)-\mathbf{A}\mathbf{S}(t)\right\|^2$$

Obviously, the estimate for the signal waveform is:

$$\hat{\mathbf{S}}(t) = \mathbf{A}^{+}\mathbf{X}(t)$$

where $\mathbf{A}^+$ is the pseudo-inverse of **A**. To calculate σ^2 it is necessary to take the derivative of the log-likelihood function and set the result equal to zero, i.e:

$$\hat{\sigma}^2 = \frac{1}{JM}\sum_{t=1}^{J}\left\|\mathbf{X}(t)-\mathbf{A}\mathbf{S}(t)\right\|^2$$

If **S**(t) is substituted in the above equation, then:

$$\hat{\sigma}^2 = \frac{1}{JM}\sum_{t=1}^{J}\left\|\mathbf{X}(t)-\mathbf{A}\mathbf{A}^{+}\mathbf{X}(t)\right\|^2 = \frac{1}{J}\mathrm{Tr}\{\mathbf{P}_{\mathbf{A}}^{\perp}\hat{\mathbf{R}}_{xx}\}$$

where $\mathbf{P}_{\mathbf{A}}^{\perp} = \mathbf{I} - \mathbf{A}\mathbf{A}^{+}$ is the orthogonal projection matrix.

The following non-linear optimization problem is then obtained as an estimator for (θ,ϕ):

$$(\hat{\theta},\hat{\phi}) = \arg\min_{\theta,\phi} \mathrm{Tr}\{\mathbf{P}^{\perp}{}_{A}\,\hat{\mathbf{R}}_{xx}\}$$

Maximum Likelihood Estimation is a parametric method and hence its resolution is not limited, as is the case for the conventional beamformer. However, a multidimensional search is required to find the estimates, resulting in a high computational complexity. The ML estimator presented here can be classified as a deterministic ML estimator, because the impinging multipath rays of both the desired signal and the interferers are modelled deterministically. It is also possible to model the interfering sources as coloured Gaussian noise. For the deterministic model, the number of signal waveform parameters grows as the number of samples increases, implying that they cannot be estimated consistently.

8.5 Conclusion.

In this section we have reviewed some of the main estimation methods that may be used to simultaneously determine the DOAs of a number of signals. In practice, however, beamforming is of limited interest in DOA estimation as its resolution is limited to that of the antenna array structure. We will, therefore, for the remainder of this study concentrate on the use of Subspace and Maximum Likelihood estimation methods to obtain the required DOAs.

9. Sensitivity Analyses of Parameter Estimation Methods

9.1 Effects of Model Errors and Sensitivity Analysis on Subspace Methods[26]

For the general model errors, the array response model can be represented as:

$$\mathbf{X}(j) = \mathbf{C} \cdot \mathbf{\Gamma} \cdot \mathbf{A}(\theta) \cdot \mathbf{S}(j) + \mathbf{N}(j)$$

where **C** is the mutual coupling matrix, which models the effect of mutual coupling between antenna sensors within the array. $\mathbf{\Gamma}$ denotes a complex diagonal matrix which includes the channel gain and phase errors such that $\Gamma_{ii} = \alpha_{ii} + j\,\phi_{ii}$.

In subspace DOA estimation methods, the array output covariance matrix $\mathbf{R}_{xx}$ can be partitioned into two subspaces, the signal subspace $\mathbf{E}_s$ and the noise subspace $\mathbf{E}_n$, using eigenvalue decomposition, such that:

$$\mathbf{R}_{xx}=\mathbf{E}_s\mathbf{\Lambda}_s\mathbf{E}_s^*+ \sigma^2 \mathbf{E}_n\mathbf{E}_n^*$$

and $R(\mathbf{E}_s) \subseteq R(\mathbf{A}(\theta))$, which means that the signal subspace $\mathbf{E}_s$ is spanned by the array manifold $\mathbf{A}(\theta)$.

When we consider array response errors, the array manifold becomes $\mathbf{A}'(\theta)$, and

$$\mathbf{A}'(\theta)=\mathbf{C} \cdot \mathbf{\Gamma} \cdot \mathbf{A}(\theta) = \mathbf{C} \cdot \alpha \cdot \phi \cdot \ \mathbf{A}(\theta)$$

where $\mathbf{A}(\theta)$ is the true array manifold; **C** is the mutual coupling matrix; α and ϕ are diagonal matrices, the elements of which represent the gain and phase of each channel respectively. Therefore, the array manifold $\mathbf{A}(\theta)$ will affect the orthogonality between the two subspaces, E_s and E_n. In particular, due to the effects of the array model response errors, the real array manifold $\mathbf{A}'(\theta)$ is different from the ideal array manifold $\mathbf{A}(\theta)$. Thus the accuracy and resolution of the DOA estimation will be degraded by the errors in the array manifold. We refer to the difference between the ideal and real array parameters as a model error. For the MUSIC algorithm, if vector γ denotes the real model parameters, e.g., channel gains $\alpha= [\alpha_1, \alpha_2, \dots, \alpha_M]$ or phase $\phi = [\phi_1, \phi_2, \dots, \phi_M]$ and γ_0 represents the nominal (ideal) parameters, the spatial spectrum of MUSIC and DOA estimation will be:

$$E(\theta;\gamma) = \frac{1}{\mathbf{A}^H(\theta;\gamma)\mathbf{E}_n(\gamma)\mathbf{E}_n(\gamma)^H\mathbf{A}(\theta;\gamma)}$$

without model errors, i.e., $\gamma = \gamma_0$, we can get the exact estimate of the true DOAs. When $\gamma \neq \gamma_0$, the peaks of $E(\theta;\gamma)$ will no longer be the true DOAs and the accuracy of DOA estimations can be degraded by even small model errors. We will, therefore, consider the effect of model errors on both accuracy and resolution of DOA estimations.

9.1.1 Effects of Model Errors on the Accuracy of DOA Estimation.

We assume that the array correlation covariance matrix R_{xx} is exactly estimated, which means having an infinite (or very large) number of independent samples (snapshots), and the effect of model errors is sufficiently small so that the MUSIC spectrum has distinct peaks. Considering only the effect of variations in real parameters, we can see how much the peaks shift due to model error effects. Let:

$$F(\theta;\gamma) = \frac{1}{E(\theta;\gamma_0)} = \mathbf{A}^H(\theta;\gamma_0)\mathbf{E}_n(\gamma_0)\mathbf{E}_n(\gamma_0)^H\mathbf{A}(\theta;\gamma_0)$$

and

$$F_1(\theta;\gamma) = \frac{\partial F(\theta;\gamma)}{\partial\theta}$$

In the presence of two sources with true DOAs, θ_1 and θ_2, we perform the first-order Taylor expansion to see how much the peak locations shift due to model errors and get the angular deviation:

$$\Delta\theta_i \overset{\Delta}{=} \theta - \theta_i = -\frac{\left.\frac{\partial F_1(\theta_i;\gamma)}{\partial\gamma}\right|_{\gamma=\gamma_0}(\gamma-\gamma_0)}{\left.\frac{\partial F_1(\theta;\gamma)}{\partial\theta}\right|_{\theta=\theta_i}}$$

$$i = 1,\ \ 2$$

where γ-γ_0 is the model error. Let us assume that:

$$\gamma - \gamma_0 = \sigma_\gamma\mu$$

where μ is a random vector with zero mean and unit variance and σ_γ is a positive scalar. Thus, we can show that:

$$E\{(\gamma - \gamma_i)\} = 0$$

and the standard deviation:

$$\mathrm{std}\{(\theta - \theta_i)\} = \frac{\left\|\left.\frac{\partial F_1(\theta_i;\gamma)}{\partial\gamma}\right|_{\gamma=\gamma_0}\right\|}{\left|\left.\frac{\partial F_1(\theta_i;\gamma)}{\partial\theta}\right|_{\theta=\theta_i}\right|}\sigma_\gamma$$

where $\|\cdot\|$ is the vector norm.

Define σ_i and σ_{DOA} as follows:

$$\sigma_i = \frac{\mathrm{std}\{(\theta - \theta_i)\}}{\sigma_\gamma} = \frac{\left\| \frac{\partial F_1(\theta_i;\gamma)}{\partial \gamma}\Big|_{\gamma=\gamma_0} \right\|}{\left| \frac{\partial F_1(\theta_i;\gamma)}{\partial \theta}\Big|_{\theta=\theta_i} \right|}, \quad \sigma_{DOA} = \sqrt{\frac{1}{N}\sum_{i=1}^{N}\sigma_i^2}$$

where σ_{DOA} represents the mean square value of DOA errors caused by modeling errors and N is the number of signals. We can see that the angular standard deviation will be increased with σ_i.

9.1.2 Effects of Model Errors on Angular Resolution.

When the model errors are sufficiently large, the algorithm will fail to resolve two or more close sources, i.e. the model errors will affect the DOA resolution. In this case, as the model errors increase the valley between two peaks will become flattened and finally the two peaks merge into one so that the algorithm loses angular resolution.

The valley bottom between the two peaks given by $E(\theta,\gamma)$ can be seen as the minimum of $E(\theta,\gamma)$ and thus we have:

$$F_1(\theta^*;\gamma) = 0,$$
$$F_2(\theta^*;\gamma) = \frac{\partial^2 F(\theta;\gamma)}{\partial \theta^2}$$

In general, the location of the valley bottom, θ^*, will change with model error, γ. This fact complicates the analysis considerably. To simplify the analysis, we assume that θ^* is constant and that $\theta^*=\theta_0$, where $\theta_0=(\theta_1+\theta_2)/2$. This enables us to study $F_2(\theta_0,\gamma)$ rather than $F_2(\theta^*(\gamma),\gamma)$. Unfortunately, this is only true for uniform circular arrays and not for uniform linear arrays in the presence of phase errors. Thus the result of the first order analysis here should be used for uniform circular arrays only.

When $\theta^*=\theta_0$ and using the first-order Taylor expansion around γ_0, the smallest norm model error which will cause the MUSIC algorithm to fail is given by:

$$\gamma - \gamma_0 = \frac{\pm F_2(\theta_0,\gamma_0)\frac{\partial F_2(\theta_0,\gamma)}{\partial \gamma}\Big|\gamma=\gamma_0}{\left\| \frac{\partial F_2(\theta_0,\gamma)}{\partial \gamma}\Big|\gamma=\gamma_0 \right\|^2}$$

and the failure threshold of the MUSIC algorithm is:

$$\sigma_{fail} = \frac{1}{\sqrt{M}}\|(\gamma - \gamma_0)\|$$

where M is the number of the sensors.

9.1.3 Conclusions from Sensitivity Analyses.

The following conclusions may be drawn from the sensitivity analyses with regard to the sensitivity parameter, σ_{DOA}, and the failure threshold, σ_{fail}:

1) σ_{DOA} as a function of the source separation -

- As the number of array elements is increased, the sensitivity parameter σ_{DOA} will be decreased.
- The sensitivity parameters for circular array gain, $\sigma^{gain}_{DOA,}$ and phase, $\sigma^{phase}_{DOA,}$ will decrease almost linearly as the source separation Δ increases, i.e. $\sigma^{gain}_{DOA} \sim 1/\Delta$, $\sigma^{phase}_{DOA} \sim 1/\Delta$.
- The sensitivity parameter for linear array gain, σ^{gain}_{DOA}, will decrease almost in the same way as in the circular array. But the sensitivity parameter for phase is very small ($\sigma^{phase}_{DOA} << 1$) and will keep constant as the source separation Δ increases.
- For two adjacent signals, the sensitivity parameters for a linear array are smaller than those for a circular array.

2) σ_{DOA} as a function of the element spacing (array aperture) -

- The sensitivity parameter for linear array phase,σ^{phase}_{DOA}, is proportional to 1/d, where d is the element spacing, and also $\sigma^{phase}_{DOA} \sim 1/\Delta$. So we have $\sigma^{phase}_{DOA} \sim 1/(d\Delta)$, where d and Δ are the element spacing and source separation respectively. Let δ be the ratio of the source separation in degrees and the beamwidth, i.e. $\delta \sim (d\Delta)$, then:

$$\sigma^{phase}_{DOA} \sim 1/\delta$$

this equation shows that if the separation between two sources is same in terms of beamwidth, a linear array will have the same phase sensitivity as a circular array and its gain sensitivity, σ^{gain}_{DOA}, will decreased as d increases in proportion to$1/d \cdot k$ ($2 \le k \le 2.5$).

- The sensitivity parameters of a circular array, σ^{gain}_{DOA} and σ^{phase}_{DOA} will decrease rapidly as the element spacing d increases, in proportion to $1/d \cdot k$ ($2 \le k \le 2.5$) also.

3) σ_{fail} as a function of source separation -

- The ways the peaks shift because of phase errors are different in linear and non-linear arrays. In a linear array phase errors cause the peaks to shift in the same direction by almost

the same amount whereas, in a non-linear array the peaks move towards each other until they eventually merge into one.

- The failure threshold σ_{fail} is approximately proportional to Δ^2, i.e., $\sigma_{fail} \sim \Delta^2$.

4) σ_{fail} as a function of element spacing -

- The gain failure threshold σ^{gain}_{fail} is approximately proportional to d^2,

  i.e., $\sigma^{gain}_{fail} \sim d^2$ and for a circular array, the phase failure threshold is given by

$$\sigma^{phase}_{fail} \sim d^k \ (2 \le k \le 3)$$

- $\sigma^{gain}_{fail} \sim \delta^2$ and $\sigma^{phase}_{fail} \sim \delta^2 d^{k-2}$ (circular array), where δ is ratio of the source separation to beamwidth.

Summarizing the results above, we get the following general conclusions:

Linear Array: It has a low sensitivity to phase errors and a larger sensitivity to gain errors, similar to a circular array. When the source separation is small the sensitivity to phase error is constant.

Circular Array: The sensitivity to both gain and phase errors is inversely proportional to the source separation and the failure threshold is approximately proportional to the square of the source separation.

As the array aperture (the number of elements) increases, the sensitivity of DOA accuracy to model errors will decrease and the failure threshold will increase.

These conclusions are only valid for the assumption that the data is infinite. In the finite data case, MUSIC is expected to fail in the presence of smaller model errors. If the SNR or the number of snapshots is too small, MUSIC will fail even in the absence of model errors.

9.2 Effects of Model Errors and Sensitivity Analysis on Maximum Likelihood Methods

The maximum likelihood DOA estimation is:

$$\hat{\theta} = \arg\max_{\theta} \mathrm{Tr}\{\mathbf{P}_{A(\theta)}\mathbf{R}_{xx}\}$$

where $P_{A(\theta)}=A(\theta)(A^H(\theta)A(\theta))^{-1} A^H(\theta)$ is a projection operator and is spanned by the columns of $A(\theta)$. The maximum likelihood estimation of θ involves multiple dimensional searching, i.e. in the N dimensional parameter space, if there are N signals coming to the array.

Here we will discuss how the ML estimate performance is affected by the DOA deviation, i.e. the error between estimates of the DOAs and the true DOAs caused by model errors.

9.2.1 The Sensitivity of DOA Estimate Accuracy to Model Errors.

In the presence of model errors, the array output covariance matrix is:

$$\mathbf{R}_{xx}(\gamma) = \mathbf{A}(\theta;\gamma)\mathbf{R}_s\mathbf{A}^H(\theta;\gamma) + \sigma^2\mathbf{I}$$

where $\mathbf{A}(\theta;\gamma)=[\mathbf{A}(\theta_1;\gamma), \mathbf{A}(\theta_2;\gamma), \ldots, \mathbf{A}(\theta_N;\gamma)]$, and γ represents the error parameter, i.e., gain, phase or sensor location errors.

The ML method is to search for the maximum of the likelihood function:

$$L(\theta,\gamma) = \mathrm{tr}(\mathbf{P}_{A(\theta;\gamma_0)}\mathbf{R}_{xx}(\gamma))$$

where $\mathbf{P}_{A(\theta;\gamma0)}=\mathbf{A}(\theta;\gamma_0)(\mathbf{A}(\theta;\gamma_0)^H\mathbf{A}(\theta;\gamma_0))^{-1}\mathbf{A}(\theta;\gamma_0)^H$. When $\gamma_0 = \gamma$, the peaks of maximum likelihood function will correspond to the true DOAs. Otherwise, if $\gamma_0 \neq \gamma_0$, the peaks will be shifted from the true DOAs.

Let the first-order derivative of the maximum likelihood function equal zero, we can then get the maximum of the maximum likelihood function. That is, let:

$$L_1(\theta;\gamma) \overset{\Delta}{=} \frac{\partial L(\theta;\gamma)}{\partial\theta}$$

then, setting $L_1(\theta;\gamma_0) = 0$, we get the following relationship for the variation in the DOA estimate versus the model errors:

$$\theta - \theta_0 = -\left(\frac{\partial L_1(\theta;\gamma)}{\partial\theta}\Big|_{\theta_0,\gamma_0}\right)^{-1}\frac{\partial L_1(\theta;\gamma)}{\partial\gamma}\Big|_{\theta_0,\gamma_0}(\gamma-\gamma_0)$$

where $(\theta - \theta_0)$ is the deviation of the estimate of the DOA and $(\gamma-\gamma_0)$ is the model error.

The norm of the DOA errors is given by:

$$\|\theta-\theta_0\|^2 = (\gamma-\gamma_0)\mathrm{M}(\gamma-\gamma_0)$$

where

$$\mathrm{M} = \frac{\partial L_1(\theta,\gamma)}{\partial\gamma}\Big|^{\mathrm{T}}_{\theta_0,\gamma_0}\left(\frac{\partial L_1(\theta,\gamma)}{\partial\theta}\Big|_{\theta_0,\gamma_0}\right)^{-\mathrm{T}}\left(\frac{\partial L_1(\theta,\gamma)}{\partial\theta}\Big|_{\theta_0,\gamma_0}\right)^{-1}\frac{\partial L_1(\theta,\gamma)}{\partial\gamma}\Big|_{\theta_0,\gamma_0}$$

Let us assume that $\gamma - \gamma_0 = \sigma_\gamma\mu$, where μ is a random vector with zero mean, unit variance and σ_γ is a positive scalar. Then

$$\mathrm{cov}\{\theta-\theta_0\} = \sigma_\gamma^2\left(\frac{\partial L_1(\theta.\gamma)}{\partial\theta}\Big|_{\theta_0,\gamma_0}\right)^{-1}\frac{\partial L_1(\theta.\gamma)}{\partial\gamma}\Big|_{\theta_0,\gamma_0}\frac{\partial L_1(\theta.\gamma)}{\partial\gamma}\Big|^{\mathrm{T}}_{\theta_0,\gamma_0}\left(\frac{\partial L_1(\theta.\gamma)}{\partial\theta}\Big|_{\theta_0,\gamma_0}\right)^{-\mathrm{T}}$$

Using the fact that tr{AB}= tr{BA}, it follows that:

$$\mathrm{tr}\{\mathrm{cov}(\theta-\theta_0)\}=\sigma_\gamma^2\mathrm{tr}\{\mathrm{M}\}$$

Note that tr{cov(θ-θ0)}/N is the average variance of the DOA errors, i.e.

$$\frac{1}{\mathrm{N}}\mathrm{tr}\{\mathrm{cov}(\theta-\theta_0)\}=\frac{1}{\mathrm{N}}\sum_{\mathrm{n=1}}^{\mathrm{N}}\mathrm{var}(\theta-\theta_0)$$

Therefore, we have the DOA sensitivity of the ML algorithm to model errors,

$$\sigma_{\mathrm{DOA}}=\sqrt{\frac{\mathrm{tr}\{\mathrm{cov}(\theta-\theta_0)\}}{\mathrm{N}\sigma_\gamma^2}}=\sqrt{\frac{\mathrm{tr}\{\mathrm{M}\}}{\mathrm{N}}}$$

and this angular deviation will increase as tr{M} increases.

9.2.2 Failure Threshold of ML Algorithm.

As the model error increases, the ML algorithm will fail to provide meaningful DOA estimates if the peaks of the maximum likelihood function occur on the failure line characterized by:

$$\theta=\alpha\mathbf{I}$$

where $\mathbf{I}=[1,1]^{\mathrm{T}}$ and α is an arbitrary scalar. We can then obtain:

$$\alpha\mathbf{I}-\theta_0=-\left(\frac{\partial \mathrm{L}_1(\theta,\gamma)}{\partial\theta}\Big|_{\theta_0,\gamma_0}\right)^{-1}\frac{\partial \mathrm{L}_1(\theta,\gamma)}{\partial\gamma}\Big|_{\theta_0,\gamma_0}(\gamma-\gamma_0)$$

This equation can be resolved non-uniquely for γ - γ0, given any value of α. We perform a singular value decomposition of $\frac{\partial \mathrm{L}_1(\theta,\gamma)}{\partial\gamma}\Big|_{\theta_0,\gamma_0}$, to give:

$$\frac{\partial \mathrm{L}_1(\theta,\gamma)}{\partial\gamma}\Big|_{\theta_0,\gamma_0}=\mathbf{U}_1\Sigma_1\mathbf{V}_1^{\mathrm{H}}$$

Define $\delta=\mathrm{V}_1^{\mathrm{H}}(\theta-\theta_0)$ and then:

$$\alpha\mathbf{I}-\theta_0=-\left(\frac{\partial \mathrm{L}_1(\theta,\gamma)}{\partial\theta}\Big|_{\theta_0,\gamma_0}\right)^{-1}\mathbf{U}_1\Sigma_1\delta$$

or:

$$\theta_0 = \left[\left(\frac{\partial L_1(\theta,\gamma)}{\partial \theta}\bigg|_{\theta_0,\gamma_0} \right)^{-1} \mathbf{U}_1 \Sigma_1 \mathbf{I} \right] \left[\frac{\delta}{\alpha} \right]$$

The minimum norm solution of this under-determined set of equations could be obtained by various matrix-solving routines. We only need to find the smallest $\|\delta\|$ and smallest $\|\gamma-\gamma_0\|$. Due to $\mathbf{V}_1$ being an orthogonal matrix, the norm of δ is same as the norm of $\gamma-\gamma_0$. Thus, if we consider the effect of model errors on each element, the failure threshold of the ML algorithm will be related to $\|\delta\|$ and we have the failure threshold of the ML algorithm as:

$$\sigma_{\text{fail}} = \frac{\|\delta\|}{\sqrt{M}}.$$

10. Selection of Estimation Method and Algorithm Development.

10.1 Selection of Estimation Method.

In section 8 of this report we reviewed the main methods of parameter estimation; beamforming, subspace-based methods and maximum-likelihood methods. In practice, however, beamforming is of limited interest in DOA estimation as its resolution is limited to that of the antenna array structure. In section 9 of this report sensitivity analyses were produced to investigate the effect of model errors on both Subspace methods and Maximum Likelihood methods. As a result of these analyses, it was decided that in the case of known frequency an ML method would be considered and for unknown frequencies subspace methods would be investigated, as these would give the best angular resolution while having a lower computational complexity than ML methods. A number of estimation algorithms using sub-space methods were considered, with special emphasis on the solution of multi-parameter estimations, and details follow in this section.

10.2 Algorithm Development.

In section 8.3 of this report we reviewed the basics of Subspace-based estimation methods with reference to the MUSIC, ESPRIT and WSF methods in particular. As part of this project work has been carried out into using various subspace methods to estimate a number of parameters simultaneously. Maximum Likelihood methods were considered in Section 8.4.

10.2.1 Maximum Likelihood Method.

We will consider an ML method to estimate the Mutual Coupling Matrix in the case of known signal frequency. For the papers of mutual coupling modeling and previous work, see [28],[30],[38],[43],[50],[51],[53],and[58].

We make the standard assumptions underlying the algorithms:

(1) The signal and noise processes are stationary and ergodic over the observation period.

(2) The columns of $\mathbf{A}(\theta)$ are linearly independent.

(3) The noise is uncorrelated with the signal, and it has zero mean value. Its covariance matrix is full rank and is known except for a multiplication constant σ^2.

(4) The total number of sources is known ($2 \le p \le M$) and the sources have the same known frequency.

(5) The MCM satisfies rank(**C**) = M which implies that rank (**CA**(**θ**)) = rank(**A**(**θ**)) = p

.

10.2.1.1 Estimation process

The algorithm proposed here consists of two estimation procedures: estimation of signal directions of arrival $\{\boldsymbol{\theta}_n\}$ and estimation of mutual coupling matrix **C**.

1. Estimation of directions of arrival $\{\boldsymbol{\theta}_n\}$

Defining:

$$Q_1 = \sum_{j=1}^{J} \left\| \mathbf{X}(j) - \mathbf{C}^0 \mathbf{A}\left(\boldsymbol{\theta}^0\right) \hat{\mathbf{S}}_0(j) \right\|^2$$

$$\hat{\mathbf{S}}_0(j) = \left(\mathbf{B}_0^H \mathbf{B}_0\right)^{-1} \mathbf{B}_0^H \mathbf{X}(j) \qquad ...(10.1)$$

where $\|\bullet\|$ denotes the Euclidean norm. J is the number of samples (snapshots). $\mathbf{B}_0 = \mathbf{C}^0\mathbf{A}(\boldsymbol{\theta}^0)$ denotes the array steering matrix with the effects of mutual coupling, $\mathbf{C}^0$ and $\boldsymbol{\theta}^0$ are the initial values of the mutual coupling matrix and DOAs respectively.

During this first step, the algorithm performs successive minimization operations on each column of $\mathbf{B}_0$ and holds all of other columns and associated components of $\hat{\mathbf{S}}_0(j)$ fixed. Suppose that we perform the minimization with respect to the k^{th} column vector, Q_1 can be written as:

$$Q_1 = \sum_{j=1}^{J} \left\| \mathbf{X}^k(j) - \mathbf{b}_0(\theta_k) \hat{\mathbf{S}}_{0k}(j) \right\|^2 \qquad ....(10.2)$$

where $\mathbf{b}_0(\theta_k)$ is the k^{th} column of $\mathbf{B}_0$, $\hat{\mathbf{S}}_{0k}(j)$ is the k^{th} component of $\hat{\mathbf{S}}_0(j)$, and $\mathbf{X}^k(j)$ is given by:

$$\mathbf{X}^k(j) = \mathbf{X}(j) - \mathbf{C}^0 \mathbf{A}\left(\boldsymbol{\theta}^0\right) \mathbf{S}_0^k(j) = \mathbf{X}(j) - \mathbf{B}_0 \mathbf{S}_0^k(j) \qquad ....(10.3)$$

where $\mathbf{S}_0^k(j)$ is a simplification of $\hat{\mathbf{S}}_0(j)$ with the k^{th} part replaced by zero.

The minimization of (10.3) with respect to $\mathbf{a}_0(\theta_k)$, using (10.1) with $\mathbf{B}_0$ replaced by $\mathbf{b}_0(\theta_k)$, is:

$$\hat{\theta}_k = \arg\min_{\theta_k} \sum_{j=1}^{J} \left\| \mathbf{X}^k(j) - \mathbf{b}_0(\theta_k) \left(\mathbf{b}_0(\theta_k)^H \mathbf{b}_0(\theta_k)\right)^{-1} \mathbf{b}_0(\theta_k)^H \mathbf{X}^k(j) \right\|^2$$

which is also equivalent to:

$$\hat{\theta}_k = \arg\max_{\theta_k} \frac{1}{M} \sum_{j=1}^{J} \left| \mathbf{X}^k(j)^H \mathbf{b}_0(\theta_k) \right|^2 \qquad ....(10.4)$$

where $M = \mathbf{b}_0(\theta_k)^H \mathbf{b}_0(\theta_k)$

To maximize (10.4), we can search over the space of $\{\theta_k\}$ and finally get the directions of arrival (DOAs) $\{\theta_n\}$. Based on these DOAs, we can reconstruct the new steering matrix $\mathbf{A}(\boldsymbol{\theta}^1)$ and put:

$$\hat{\mathbf{S}}_{01}(j) = \left(\mathbf{B}_{01}^H \mathbf{B}_{01}\right)^{-1} \mathbf{B}_{01}^H \mathbf{X}(j)$$

where $\mathbf{B}_{01} = \mathbf{C}^0 \mathbf{A}(\boldsymbol{\theta}^1)$, $\boldsymbol{\theta}^1 = [\hat{\theta}_1\ \hat{\theta}_2 \cdots \hat{\theta}_p]$. The initial mutual coupling matrix $\mathbf{C}^0$ of this first step is fixed and we have to iterate and update **C** at the second step to approach the true DOAs and MCM **C**.

2. Estimation of the mutual coupling matrix **C.**

At this step, we can estimate the MCM with the DOAs $\{\theta_n\}$ provided by the last step. Since we have new values for $\mathbf{S}_{01}(j)$ and $\mathbf{A}(\theta^1)$, Q can be written as:

$$Q = \sum_{j=1}^{J} \left\| \mathbf{X}(j) - \mathbf{C}\mathbf{A}(\boldsymbol{\theta}^1)\hat{\mathbf{S}}_{01}(j) \right\|^2 \qquad \ldots.(10.5)$$

Because **C** is an M ×M banded complex symmetric Toeplitz matrix in the case of a uniform linear array or an M ×M complex circulant matrix in the case of a uniform circular array and $\mathbf{A}(\boldsymbol{\theta}^1)\mathbf{S}_{01}(j)$ is an M ×1 complex vector, the following two lemma [11?] will be useful.

Lemma 10.1 For any M ×1 complex vector **x** and any M ×M banded complex symmetric Toeplitz matrix **B**:

$$\mathbf{B}.\mathbf{x} = \mathbf{Q}_1(x).\mathbf{b}$$

where the L ×1 vector **b** is given by:

$$b_i = B_{1i}, \quad i = 1, 2, \ldots, L$$

where L is the highest super-diagonal that is different from zero. The M ×L matrix $\mathbf{Q}_1(x)$ is given by the sum of the following matrices:

$$[\mathbf{T}_1]_{pq} = \begin{cases} x_{p+q-1} & p+q \le M-1 \\ 0 & \text{otherwise} \end{cases}$$

$$[\mathbf{T}_2]_{pq} = \begin{cases} x_{p-q+1} & p \ge q \ge 2 \\ 0 & \text{otherwise} \end{cases}$$

Lemma 10.2 For any M ×1 complex vector **x** and any M ×M complex symmetric circulant matrix **A**:

$$\mathbf{A}.\mathbf{x} = \mathbf{Q}_2(x).\mathbf{a}$$

where the component of the L ×1 vector **a** is given by:

$$a_i = A_{1i}, \quad i = 1, 2, \ldots, L$$

where L = M/2 +1when M is even and L = (M +1)/2 when M is odd.

The M ×L matrix $\mathbf{Q}_2(x)$ is given by the sum of the following four M ×L matrices:

$$[\mathbf{T}_1]_{pq} = \begin{cases} x_{p+q-1} & p+q \le M-1 \\ 0 & \text{otherwise} \end{cases}$$

$$[\mathbf{T}_2]_{pq} = \begin{cases} x_{p-q+1} & p \ge q \ge 2 \\ 0 & \text{otherwise} \end{cases}$$

$$[\mathbf{T}_3]_{pq} = \begin{cases} x_{M+1+p-q} & p < q \le 1 \\ 0 & \text{otherwise} \end{cases}$$

$$[\mathbf{T}_4]_{pq} = \begin{cases} x_{p+q-M-1} & 2 \le q \le l, p+q \ge M+2 \\ 0 & \text{otherwise} \end{cases}$$

where l = M/2 for even M and l = (M +1)/2 for odd M .

Using Lemma 10.1 or Lemma 10.2, depending on the array configuration, we have:

$$\mathbf{C}\mathbf{A}(\boldsymbol{\theta}^1)\hat{\mathbf{S}}_{01}(j) = \mathbf{C}\mathbf{W}$$

and:

$$\mathbf{C}\mathbf{W} = \mathbf{T}_{MxL}\mathbf{G}_{Lx1}$$

where the L ×1 vector **G** is given by:

$$G_i = C_{1i}, \qquad i = 1, 2, \bullet\bullet\bullet, L$$

by letting **CW** = **TG**, we can place the unknowns in the L ×1 vector **G** and the known values in the M ×L matrix **T**. Thus, (10.5) can be rewritten as:

$$Q = \sum_{j=1}^{J} \left\| \mathbf{X}(j) - \mathbf{T}\mathbf{G} \right\|^2$$

and vector **G** as:

$$\mathbf{G} = \frac{1}{J}\sum_{j=1}^{J} \left(\mathbf{T}^H\mathbf{T}\right)^{-1}\mathbf{T}^H\mathbf{X}(j)$$

and we can now reconstruct the MCM **C** from vector **G**:

$$\mathbf{C} = \begin{cases} \text{Toeplitz}(\mathbf{G}) & \text{For ULA} \\ \text{Circulant}(\mathbf{G}) & \text{For UCA} \end{cases}$$

10.2.1.2 Convergence check

During both the estimation steps, we check the convergence of (10.2) and (10.5). When both $Q_1^{(k-1)} - Q_1^{(k)} \leq \varepsilon$ and $Q^{(k-1)} - Q^{(k)} \leq \varepsilon$ (ε is a given threshold), the algorithm has converged and we get the estimation of the DOAs and the MCM **C** . Otherwise, the algorithm will be repeated between the two steps until Q_1 and Q converge. Note that the cost functions, Q_1 ($Q_1 \geq 0$) and Q ($Q \geq 0$), are convergent series and the convergence of both is guaranteed.

10.2.2 Iterative MUSIC Method

In [9], an iterative subspace method based on the MUSIC algorithm was presented to deal with the estimation of DOAs and unknown mutual coupling as well as gain and phase errors. The algorithm first searches for peaks in the MUSIC spectrum, similarly to the original MUSIC algorithm without mutual coupling, to get an estimation of the DOAs and then estimates the mutual coupling. This procedure is repeated several times and becomes a two-step iterative optimization for the cost function [9]:

$$J_c = \sum_{p=1}^{N} \left\| \hat{\mathbf{E}}_n \mathbf{C}\boldsymbol{\Gamma}\mathbf{a}(\theta_p) \right\|^2$$

where $\hat{\mathbf{E}}_n$ are the noise eigenvectors, eigen-decomposed from the estimation of the data covariance matrix **R**, **C** is the mutual coupling matrix and $\boldsymbol{\Gamma}$ is the gain and phase matrix, in this case it is assumed that $\boldsymbol{\Gamma} = \mathbf{I}$ as only the mutual coupling is being considered.

Step 1: Estimating the DOAs.

Search for the N highest peaks of the MUSIC spectrum defined by:

$$P_{music}(\theta) = \left\| \hat{\mathbf{E}}_n \mathbf{C}\mathbf{a}(\theta) \right\|^{-2}$$

where the initial mutual coupling matrix **C** can initially be chosen as an identity matrix and the estimations of the DOAs are associated with the N highest peaks in the spectrum.

Step 2: Estimating the Mutual Coupling Matrix

In this step, the vector $\mathbf{a}(\theta_p)$ in the cost function J_c will be updated by the estimated DOAs, $\{\theta_p\}(p = 1, 2, \ldots, N)$, and then the mutual coupling matrix **C** will be estimated by minimizing the cost function J_c .

It can be shown that for a Uniform Linear array (ULA) the MCM, **C**, is Toeplitz and for a Uniform Circular Array (UCA) the MCM is Circulant. The cost function J_c can then be written as:

$$J_c = \sum_{p=1}^{N} \mathbf{a}(\theta_p)^H \mathbf{C}^H \hat{\mathbf{E}}_n \hat{\mathbf{E}}_n^H \mathbf{C}\mathbf{a}(\theta_p)$$
$$= \mathbf{c}^H \left\{ \sum_{p=1}^{N} \mathbf{Q}(p)^H \hat{\mathbf{E}}_n \hat{\mathbf{E}}_n^H \mathbf{Q}(p) \right\} \mathbf{c}$$

where:

$$\mathbf{Q}(p) = \mathbf{Q}(\mathbf{a}(\theta_p)) \quad \text{and } c_i = C_{1i}, \ i = 1,2,\ldots,L$$

and $\mathbf{Q}(\mathbf{X})$ and L are dependent on the array configuration.

The minimization of cost function J_c is a quadratic minimization problem under a linear constrain where the MCM **C** is assumed to be unity on the main diagonal (C_{ii} =1). Thus using Lagrangian multipliers, the constrained minimization problem can be solved as:

$$\hat{\mathbf{c}} = \mathbf{G}^{-1}\mathbf{W}\left(\mathbf{W}^T\mathbf{G}^{-1}\mathbf{W}\right)^{-1}$$

where **G** is the matrix:

$$\mathbf{G} = \sum_{p=1}^{N} \mathbf{Q}(p)^H \hat{\mathbf{E}}_n \hat{\mathbf{E}}_n^H \mathbf{Q}(p)$$

and vector **W** = [1 0 •••0] represents the linear constraint.

Finally, the MCM **C** can be reconstructed from the estimated vector $\hat{\mathbf{c}}$. Note that the cost function J_c will be decreased at each iteration and the convergence of the algorithm is guaranteed.

10.2.3 Separable Sub-space Method

A following method for the joint estimation of signal frequencies, DOAs and sensor mutual coupling was presented as a paper at the IEEE 34th Asilomar Conference on Signals, Systems and Computers, October 29 - November 1, 2000, in Pacific Grove, California [10]. This paper is attached to this report as Appendix A.

Consider an array composed of M sensors with each sensor output being fed to a tap-delay-line with m taps. The delay between adjacent taps is t_0. Let $\mathbf{X}_l(t)$, (l =1 ,2 , •••,M), denote the output of the l^{th} sensor at time t and $\mathbf{X}(t) = [x(t), \bullet\bullet\bullet, x(t-(m-1)t_0)]^T$.

Assume that p narrow-band sources with different frequencies and directions impinge on the array and the incoming signals can be divided into D groups according to their wavelength, i.e:

$$p = \sum_{k=1}^{D} p_k$$

where p_k is the number of signals, from different directions, in the k^{th} group, and whose wavelength is λ_k (k =1 ,2 , •••,D).

The l^{th} sensor (l =1 ,2 , •••,M) output vector maybe written as:

$$\mathbf{X}_l(t) = \sum_{k=1}^{D}\sum_{i=1}^{M}\left(C_{l,i}(\omega_k)\mathbf{a}(\omega_k)\mathbf{b}_i(\theta_k)\right)\mathbf{S}_k(t) + \mathbf{N}_l(t)$$

$$(k = 1, 2, \bullet\bullet\bullet, D,\ i = 1, 2, \bullet\bullet\bullet, M)$$

where, $\mathbf{b}_i(\theta_k) = [\exp(-j\omega_k \tau_i(\theta_{k,1})) \bullet\bullet\bullet \exp(-j\omega_k \tau_i(\theta_{k,pk}))]$ is a $1 \times p_k$ spatial steering vector; $\mathbf{a}(\omega_k) = [1 \quad \exp(-j\omega_k t_0) \bullet\bullet\bullet \exp(-j\omega_k (m-1)t_0)]^T$ is an $m \times 1$ temporal steering vector; $C_{l,i}(\omega_k)$ is the $(l,i)^{th}$ entry in the MCM which represents the mutual coupling effect from other sensors on the l^{th} sensor; $\mathbf{S}_k(t) = [S_{k,1}(t) \bullet\bullet\bullet S_{k,pk}(t)]^T$ is a $p_k \times 1$ signal vector from the k^{th} group of narrow band sources and $\mathbf{N}_l = [N_l(t) \bullet\bullet\bullet N_l(t-(m-1)t_0)]^T$ is an $m \times 1$ additive noise vector for the l^{th} sensor.

Therefore, the array data model can be described as follows:

$$\mathbf{X}(t) = \left[\mathbf{X}_1(t)^T \quad \mathbf{X}_2(t)^T \quad \cdots \quad \mathbf{X}_M(t)^T\right]^T$$
$$= \sum_{k=1}^{D}\left(\mathbf{C}(\omega_k)\mathbf{B}(\theta_k)\right) \otimes \left(\mathbf{a}(\omega_k)\mathbf{S}_k(t)\right) + \mathbf{N}(t)$$

where:

$$\mathbf{B}(\theta_k) = \begin{bmatrix} \mathbf{b}_1(\theta_k) \\ \vdots \\ \mathbf{b}_M(\theta_k) \end{bmatrix}$$

is an $M \times p_k$ spatial steering matrix; $\mathbf{N}(t) = [\mathbf{N}_1(t)^T \quad \mathbf{N}_2(t)^T \bullet\bullet\bullet \mathbf{N}_M(t)^T]^T$ is a $Mm \times 1$ additive white Gaussian noise matrix; the symbol $\otimes$ denotes the Kronecker product and $\mathbf{C}(\omega_k)$ (k = 1, 2, •••, D) is the $M \times M$ MCM. For a ULA or UCA, $\mathbf{C}(\omega_k)$ is either a Toeplitz matrix or a circulant matrix, respectively [9].

10.2.3.1 Subspace decompositions.

Assume that the number of signals p and the number of frequency groups, D, are known.

Define:

$$\mathbf{r}'_h = \frac{1}{M}\sum_{l=1}^{M} E\left[x_l(t-(h-1)t_0)\mathbf{X}_l(t)^H\right]$$
$$(h = 1,\quad 2,\quad \cdots,\quad D)$$
$$\boldsymbol{\eta}'_l = \frac{1}{m}\sum_{h=1}^{m} E\left[y_l(t-(h-1)t_0)\mathbf{Y}(t-(h-1)t_0)^H\right]$$
$$(l = 1,\quad 2,\quad \cdots,\quad p)$$

where:

$$y_l(t-(h-1)t_0) = (\mathbf{X}_l(t))_h = x_l(t-(h-1)t_0)$$

$$\mathbf{Y}(t-(h-1)t_0) = [y_1(t-(h-1)t_0) \quad y_2(t-(h-1)t_0) \quad \cdots \quad y_M(t-(h-1)t_0)]^T$$
$$= [x_1(t-(h-1)t_0) \quad x_2(t-(h-1)t_0) \quad \cdots \quad x_M(t-(h-1)t_0)]^T$$

and E (•) denotes statistical expectation. $\{\mathbf{r}'_h\}_{h=1}^{D}$ and $\{\boldsymbol{\eta}'_l\}_{l=1}^{p}$ are the frequency and the direction vectors respectively. The range spaces spanned by the columns of these vectors are contained or are equal to the range spaces of $\mathbf{a}(\omega)$ and $\mathbf{B}(\theta)$, respectively. We have:

$$R(\mathbf{r}'_h) \subseteq R(\mathbf{a}(\omega)), \qquad R(\boldsymbol{\eta}'_l) \subseteq R(\mathbf{B}(\theta))$$

and:

$$N(\mathbf{r}'_h) \perp R(\mathbf{a}(\omega)), \qquad N(\boldsymbol{\eta}'_l) = R(\mathbf{B}(\theta))$$

where R (•) and N (•) denote the range space and null space. As is well known, subspace methods are based on the above geometrical relationships. Therefore, we may use correlation processing, in spatial and temporal dimensions respectively, to get the estimates of $\{\mathbf{r}'_h\}_{h=1}^{D}$ and $\{\boldsymbol{\eta}'_l\}_{l=1}^{p}$ and then compute their null subspaces. Finally, the frequencies, DOAs and the MCM can be estimated with subspace methods by searching corresponding spaces.

10.2.3.2 Estimation algorithm.

Step 1. Frequency Estimation.

(1) Estimation of the frequency vectors $\mathbf{r}'_h$ and $\mathbf{r}_h$:

$$\hat{\mathbf{r}}'_h = \frac{1}{M}\sum_{l=1}^{M}\frac{1}{N}\sum_{t=1}^{N} x_l(t-(h-1)t_0)\mathbf{X}_l(t)^H$$
$$\hat{\mathbf{r}}_h = \left(\hat{\mathbf{r}}'_h - \hat{\sigma}^2\mathbf{e}_h\right)^H$$

where:

$$\mathbf{e}_h = \left[\underbrace{0 \quad \cdots \quad 0}_{(h-1)} \quad 1 \quad 0 \quad \cdots \quad 0 \right], \qquad (h = 1, \quad 2, \quad \cdots, \quad D)$$

$\hat{\sigma}^2$ is the estimate of the noise variance and N is the number of samples.

(2) Gram-Schmidt (GS) orthogonalization and formation of the temporal projection matrix $\mathbf{P}_\omega$:

From the vector $\{\mathbf{r}'_h\}_{h=1}^{D}$, we can get D orthogonal vectors $\{\mathbf{q}_k\}$, (k = 1, …, D), via GS orthogonalization. Let $\mathbf{Q}_\omega = [\mathbf{q}_1, \mathbf{q}_2, \bullet\bullet\bullet, \mathbf{q}_D]$, then compute the temporal projection matrix $\mathbf{P}_\omega = \mathbf{I} - \mathbf{Q}_\omega \mathbf{Q}_\omega^H$, which spans the null space of $\{\mathbf{a}(\omega_k)\}$, (k = 1, …, D).

(3) Estimate the unknown frequencies with the temporal projection matrix $\mathbf{P}_\omega$:

The frequencies $\{\omega_k\}$, (k = 1, …, D), are estimated as the D largest peaks of the function:

$$P(\omega) = \frac{1}{\mathbf{a}(\omega)^H \mathbf{P}_\omega \mathbf{a}(\omega)}$$

by searching over the frequency sector of interest.

Step 2. Direction and Mutual Coupling Estimation

(1) Estimation of direction vectors, $\boldsymbol{\eta}'_l$ and $\boldsymbol{\eta}_l$:

$$\hat{\boldsymbol{\eta}}'_l = \frac{1}{m}\sum_{h=1}^{m} \frac{1}{N}\sum_{t=1}^{N} y_l(t-(h-1)t_0)\mathbf{Y}(t-(h-1)t_0)^H$$

$$\hat{\boldsymbol{\eta}}_l = \left(\hat{\boldsymbol{\eta}}'_l - \hat{\sigma}^2 \mathbf{e}_l\right)^H$$

where:

$$\mathbf{e}_l = \left[\underbrace{0 \quad \cdots \quad 0}_{(l-1)} \quad 1 \quad 0 \quad \cdots \quad 0 \right], \qquad (l = 1, \quad 2, \quad \cdots, \quad p)$$

(2) By GS orthogonalization of $\{\hat{\boldsymbol{\eta}}_l\}_{l=1}^{p}$, the p orthogonal vectors, $\{\boldsymbol{\zeta}_l\}_{l=1}^{p}$ and spatial orthogonal projection matrix $\mathbf{P}_\theta = \mathbf{I} - \mathbf{Q}_\theta \mathbf{Q}_\theta^H$ are obtained, where $\mathbf{Q}_\theta = [\boldsymbol{\zeta}_1 \ \boldsymbol{\zeta}_2 \ \ldots \ \boldsymbol{\zeta}_p]$.

(3) For each frequency $\{\omega_k\}$, (k = 1, 2, …, D), estimated in Step 1, the directions $\theta_{i\,k}$, ($i_k = 1, 2, \bullet\bullet\bullet, p_k$) and mutual coupling matrix $\mathbf{C}(\omega_k)$ can be estimated by using the Iterative MUSIC method described in section 10.2.2 with the following equations:

$$P(\theta) = \left(\mathbf{B}(\theta)^H \mathbf{C}(\omega_k)^H \mathbf{P}_\theta \mathbf{C}(\omega_k)\mathbf{B}(\theta)\right)^{-1}$$
$$\hat{\mathbf{c}}(\omega_k) = \left(\mathbf{G}(\omega_k)^{-1}\mathbf{w}\right)\left(\mathbf{w}^H \mathbf{G}(\omega_k)^{-1}\mathbf{w}\right)^{-1}$$

where $\mathbf{G}(\omega_k) = \sum_{i_k=1}^{p_k} \mathbf{D}(\theta_{i_k})^H \mathbf{P}_\theta \mathbf{D}(\theta_{i_k})$ and $\mathbf{w} = [1, 0, \bullet\bullet\bullet, 0]^T$. Using the properties of Toeplitz and Circulant matrices and Lemmas 10.1 and 10.2, matrix $\mathbf{D}(\theta_{i_k})$ can be calculated [11] by letting $\mathbf{C}(\omega_k)\mathbf{B}(\theta_{i_k}) = \mathbf{D}(\theta_{i_k})\mathbf{c}$, *i.e.*, the unknowns are placed in vector **c** and the known values in the matrix **D**.

10.2.4 Alternating Iterative Method.

This section presents an alternating iterative based approach for the estimation of DOAs, signal frequencies and corresponding array sensor gain/phase errors from the received signals. The previous work, see [27],[41],[44],[47],[55], and [59]. The approach consists of two parts: first estimate signal frequencies and then estimate the directions of arrival and the corresponding gain/phase errors. Since this multiple parameter estimation procedure is a non-linear optimisation problem, the alternating iterativeness will be used to get the solution, *i.e*, one can first estimate frequencies and DOAs based on supposing that the array gain/phase errors are initially known, which can be determined from nominal or recently measured values, and then estimate the array gain/phase errors with the estimated frequencies and DOAs. This procedure will be repeated until the cost function reaches a minimum.

10.2.4.1 Estimation procedure

1) Estimation of the signal frequencies ω_k , (k = 1 … D).

Applying conventional frequency estimation methods, such as a periodogram or other temporal spectral estimation methods [12], to the received signal matrix **X**, D signal frequencies can be estimated. For each estimated signal frequency, one can then estimate the signal directions of arrival and the gain/phase matrix with the following iterative procedures.

2) Estimation of the DOAs θ_{kn} ,(n = 1 … p_k).

Suppose that the initial gain/phase matrix $\mathbf{\Gamma}_k^{(0)}$ is known; this could be based on either the nominal gain/phase values or on any recent calibration information. For the i^{th} iteration, the azimuth and elevation space, $\theta_k = [\theta, \phi]^T$, are searched with:

$$D^{(i)}(\theta_k) = \frac{1}{\left\| \mathbf{E}_n \mathbf{\Gamma}_k^{(i)} \mathbf{a}(\theta_k) \right\|^2} \quad \ldots(10.6)$$
$$k = 1, \quad 2, \quad \cdots, \quad D$$

where $\mathbf{E}_n$ is a matrix whose columns are the eigenvectors corresponding to the smallest eigenvalues of covariance matrix $\mathbf{R}_x = E\{ \mathbf{X}\,\mathbf{X}^H \}$. Then, the p_k peaks indicate the signal directions of arrival, $\left\{ \hat{\theta}_{k_n}^{(i)} \right\}_{n=1}^{p_k}$, at the i^{th} iteration.

3) Estimation of the gain/phase matrix $\mathbf{\Gamma}_k$.

When the DOAs with frequency ω_k have been estimated, the estimation of the gain/phase matrix at that frequency, $\mathbf{\Gamma}_k$, becomes a constraint optimisation problem for the cost function:

$$L_k = \sum_{n=1}^{p_k} \left\| \mathbf{E}_n^H \mathbf{\Gamma}_k \mathbf{a}(\omega_k, \theta_{k_n}) \right\|^2$$
$$k = 1, \quad 2, \quad \cdots, \quad D$$

Since the gain/phase error matrix, $\mathbf{\Gamma}_k$, is an M x M diagonal matrix and $\mathbf{a}(\omega_k, \theta_{kn})$ is an M x 1 vector, we have:

$$\mathbf{\Gamma}_k \mathbf{a}(\omega_k, \theta_{k_n}) = \mathbf{Q}(\omega_k, \theta_{k_n}) \boldsymbol{\delta}_k$$

where $\boldsymbol{\delta}_k$ is a vector composed of the diagonal elements of $\mathbf{\Gamma}_k$ and matrix $\mathbf{Q}(\omega_k, \theta_{kn})$ is an M x M diagonal matrix whose diagonal elements are the elements of vector $\mathbf{a}(\omega_k, \boldsymbol{\theta}_{kn})$.

Therefore, the cost function L_k can be rewritten as:

$$L_k = \sum_{n=1}^{P_k} \mathbf{a}(\omega_k, \theta_{k_n})^H \mathbf{\Gamma}_k \mathbf{E}_n^H \mathbf{E}_n \mathbf{\Gamma}_k \mathbf{a}(\omega_k, \theta_{k_n})$$
$$= \boldsymbol{\delta}_k^H \left\{ \sum_{n=1}^{P_k} \mathbf{Q}(\omega_k, \theta_{k_n}) \mathbf{E}_n^H \mathbf{E}_n \mathbf{Q}(\omega_k, \theta_{k_n}) \right\} \boldsymbol{\delta}_k$$

with the optimisation constraint:

$$\boldsymbol{\delta}_k \mathbf{w} = 1, \qquad \mathbf{w} = [1 \quad 0 \quad \cdots \quad 0]^T$$

The result of this minimization is given by:

$$\boldsymbol{\delta}_k^{(\text{update})} = \mathbf{Z}_k^{-1}\mathbf{w} / \left(\mathbf{w}^T \mathbf{Z}_k^{-1}\mathbf{w}\right) \quad \ldots(10.7)$$

where:

$$\mathbf{Z}_k = \sum_{n=1}^{P_k} \mathbf{Q}\left(\omega_k, \theta_{k_n}\right) \mathbf{E}_n^H \mathbf{E}_n \mathbf{Q}\left(\omega_k, \theta_{k_n}\right)$$

and finally:

$$\boldsymbol{\Gamma}_k^{(\text{update})} = \text{diag}\left\{\boldsymbol{\delta}_k^{(\text{update})}\right\} \quad \ldots(10.8)$$

10.2.4.2 Algorithm summary.

The alternating iterative method can be summarized as:

(1) Estimation of frequencies with conventional frequency estimation methods.

(2) Estimation of data covariance matrix:

$$\hat{\mathbf{R}}_x = \frac{1}{J}\sum_{j=1}^{J} \mathbf{X}_j \mathbf{X}_j^H$$

(3) Eigenvalue decomposition (EVD) of the covariance matrix $\mathbf{R}_x$ to separated signal subspace $\mathbf{E}_s$ and noise subspace $\mathbf{E}_n$.

(4) Set i = 0 and set initial value of the gain/phase matrix $\boldsymbol{\Gamma}_k$ for each frequency ω_k, where k = 1, 2, …, D.

(5) For each estimated frequency ω_k, the estimation of the directions of arrival can be calculated using (10.6), where the p_k peaks indicate the directions of arrival, $\theta_{kn}^{(i)}$ (n=1, …, p_k).

(6) Using (10.7) and (10.8), estimate the gain/phase matrix $\boldsymbol{\Gamma}_k^{(i)}$.

(7) Compute the cost function $L_k^{(i)}$ and the cost function $L = \sum_{k=1}^{D} L_k$. Repeat steps (4) - (7) with updated DOAs $\boldsymbol{\theta}_{kn}^{(i)}$ (n = 1, …,p_k) and gain/phase matrix $\boldsymbol{\Gamma}_k^{(i)}$ until the reduction in cost function $L_k^{(i)} - L_k^{(i+1)} \le \varepsilon$, (where ε is a given threshold). For D frequencies, this procedure will be repeated D times until the cost function L reaches a minimum.

As the above estimation is a nonlinear alternative iterative optimisation procedure, whether or not the iterative procedure converges to the global optimum depends on the choice of initial values. This method may converge to a local optimum. To improve the performance of convergence, we will introduce a simulated annealing algorithm and then present a global optimisation method for the estimation of DOAs, frequencies and array gain/phase error.

10.2.5 Global Optimisation Based on Simulated Annealing

The joint DOA and frequency dependent gain/phase error estimation algorithm proposed here is based on simulated annealing and consists of two parts. The first is to form a projection matrix from the covariance matrix and to then construct a spectral estimation matrix and cost function from the projection matrix. The second is to minimize the cost function by simulated annealing.

10.2.5.1 The projection matrix and spectral-estimation matrix.

In Section 7 we have described the modified frequency-direction array response model with unknown gain and phase errors. Our work here is first to form an orthogonal projection matrix **P** from the covariance matrix $\mathbf{R}_x$. Such a projection matrix can be formed from the p principal eigenvectors of the covariance matrix.

On obtaining the projection matrix **P**, we can construct a spectrum-estimation matrix:

$$\mathbf{S}(\Gamma,\omega,\theta)=\frac{1}{\mathrm{Tr}\left(\left[\mathbf{PA}'(\boldsymbol{\omega},\boldsymbol{\theta})\right]\left[\mathbf{PA}'(\boldsymbol{\omega},\boldsymbol{\theta})^{\mathrm{H}}\right]\right)}$$

where:

$$\mathbf{A}'(\boldsymbol{\omega},\boldsymbol{\theta})=\left[\boldsymbol{\Gamma}(\omega_1)\mathbf{A}(\omega_1,\theta_1)\vdots\boldsymbol{\Gamma}(\omega_2)\mathbf{A}(\omega_2,\theta_2)\vdots\cdots\vdots\boldsymbol{\Gamma}(\omega_{\mathrm{D}})\mathbf{A}(\omega_{\mathrm{D}},\theta_{\mathrm{D}})\right]$$

is the modified frequency-direction steering matrix with the sensor gain/phase errors.

Because the trace of the spectral-estimation matrix contains information for the signal frequencies, DOAs and array gain/phase errors, the estimation of all these variables may be obtained by minimizing the cost function:

$$\begin{aligned}\mathbf{L}(\Gamma,\omega,\theta)&=\mathrm{Tr}\left(\left[\mathbf{PA}'(\boldsymbol{\omega},\boldsymbol{\theta})\right]\left[\mathbf{PA}'(\boldsymbol{\omega},\boldsymbol{\theta})^{\mathrm{H}}\right]\right)\\&=\sum_{k=1}^{D}\mathrm{Tr}\left(\left[\mathbf{PA}'(\omega_k,\boldsymbol{\theta})\right]\left[\mathbf{PA}'(\omega_k,\boldsymbol{\theta})^{\mathrm{H}}\right]\right)\end{aligned}$$

The minimization of this cost function is a non-linear optimisation problem. We will utilize simulated annealing to perform a global optimisation. Regarding simulated annealing and its applications, see papers, e.g [15],[18],[23],[36],[47],[49], [57]and [60].

10.2.5.2 Global optimisation procedure

As has been described above, the proposed algorithm consists of two parts; forming the cost function from the spectrum-estimation matrix and then using simulated annealing to minimize the cost function. The global minimization procedure by simulated annealing can be outlined as follows:

Initialization

set annealing schedule $(T_0, n_0)\cdots(T_f, n_f)$ *;*

generate $(\Gamma^0, \omega^0, \theta^0)$ *randomly;*

compute $L(\Gamma^0, \omega^0, \theta^0)$ *;*

where

$$L(\Gamma, \omega, \theta) = \sum_{k=1}^{D} \mathrm{tr}\left\{[\mathbf{P}\Gamma(\omega_k)\mathbf{A}(\omega_k, \theta_k)][\mathbf{P}\Gamma(\omega_k)\mathbf{A}(\omega_k, \theta_k)]^H\right\}$$

outer loop

set i=1*;*

inner loop

from k=1 to n_i *;*

generate random perturb $(\Gamma^k, \omega^k, \theta^k)$ *;*

compute $L(\Gamma^k, \omega^k, \theta^k)$ *;*

generate random number ξ *with* (0 , 1)

uniform distribution ;

if $\xi < p$ *or if* $\Delta > 0$ *, accept* $(\Gamma^k, \omega^k, \theta^k)$ *;*

where

$p = \min(1, \exp(-\Delta/T_i))$,

$\Delta = L(\Gamma^{k-1}, \omega^{k-1}, \theta^{k-1}) - L(\Gamma^k, \omega^k, \theta^k)$,

otherwise ,reject;

end of inner loop;

set $L(\Gamma^k, \omega^k, \theta^k)$ *generated by inner loop to*

$L(\Gamma^0, \omega^0, \theta^0)$ *;*

$i = i + 1$ *;*

repeat until i > f *or according to other stop criterion to end outer loop.*

In the above procedure, the kernel of the simulated annealing algorithm is to determine the annealing schedule $\{(T_0, n_0)\cdots(T_f, n_f)\}$.; where T_0 is the initial temperature, $T_i (i = 1,2,\cdots,f)$ is the current control temperature, and $n_i (i = 1,2,\cdots,f)$ is the cycle number of the inner loop.

The random perturbation $(\Gamma^k, \omega^k, \theta^k)$ generated at the k^{th} repetition will be accepted with probability p:

$$p = \min(1, \exp(-\Delta/T_i))$$

where:

$$\Delta = L(\Gamma^{k-1}, \omega^{k-1}, \theta^{k-1}) - L(\Gamma^k, \omega^k, \theta^k)$$

and:

$$L(\Gamma, \omega, \theta) = \sum_{k=1}^{D} \mathrm{tr}\left\{[\mathbf{P}\Gamma(\omega_k)\mathbf{A}(\omega_k, \theta_k)][\mathbf{P}\Gamma(\omega_k)\mathbf{A}(\omega_k, \theta_k)]^H\right\}$$

If $\Delta > 0$, then accept $L(\Gamma^k, \omega^k, \theta^k)$, otherwise accept $L(\Gamma^k, \omega^k, \theta^k)$ with probability $p = \exp(-\Delta/T_i)$.

Repeating the above procedure can reach the global minimum (or approximately global minimum) and the proof of convergence can be seen in [13, 14].

10.2.5.3 Algorithm summary.

The main procedure of the proposed algorithm may be summarized as follows:

1) Initialization :

Select the initial values for the signal frequencies $\{\omega^0\}$, directions $\{\theta^0\}$, and array error matrix $\{\Gamma^0\}$. Usually the initial values can be selected randomly or from the last measured values.

2) Use all the available data vectors to estimate the data covariance matrix :

$$\mathbf{R}_x = \frac{1}{J}\sum_{j=1}^{J} \mathbf{X}(j)\mathbf{X}(j)^H \qquad (j = 1, 2, \ldots, J)$$

where J is the number of samples.

3) Form the orthogonal projection matrix **P** using eigenvalue decomposition (EVD) of the data covariance matrix $\mathbf{R}_x$.

4) Construct the spectral-estimation matrix **S**:

$$\mathbf{S}(\Gamma, \omega, \theta) = \frac{1}{\mathrm{tr}([\mathbf{PA}'(\omega, \theta)][\mathbf{PA}'(\omega, \theta)]^H)}$$

and the cost function:

$$L(\Gamma,\omega,\theta) = \frac{1}{[\mathbf{S}(\Gamma,\omega,\theta)]} = \mathrm{tr}\left\{[\mathbf{PA'}(\boldsymbol{\omega},\boldsymbol{\theta})][\mathbf{PA'}(\boldsymbol{\omega},\boldsymbol{\theta})]^{H}\right\}$$
$$= \sum_{k=1}^{D} \mathrm{tr}\left\{[\mathbf{P\Gamma}(\omega_{,k})\mathbf{A}(\omega_k,\boldsymbol{\theta})][\mathbf{P\Gamma}(\omega_k)\mathbf{A}(\omega_k,\boldsymbol{\theta})]^{H}\right\}$$

5) Search (Γ,ω,θ) by simulated annealing to minimize the cost function and get the estimation of the signal frequencies, directions of arrival and array sensor errors (gains and phases).

11. Simulation Results.

11.1 Convergence Properties.

As convergence is an important property for iterative estimation methods, the convergence rates of the ML method of Section 10.2.1 and the IMUSIC method of section 10.2.2 are compared in the first example. Consider a uniform linear array with 8 sensors, each sensor separated by λ/2, with 2 equi-power narrow-band sources of known frequency located in the far field of the array at directions $\theta_1 = 30^\circ$, $\theta_2 = 45^\circ$. The signals are assumed to be uncorrelated. Additive noise is injected with a SNR of 30dB referenced to each signal source, *i.e.*,

$$\mathbf{P}/\sigma^2 = 10^{30/10}\mathbf{I}_2$$

500 snapshots of array data are accumulated. The initial values for the DOAs were chosen as $\theta_1 = 35^\circ$, $\theta_2 = 50^\circ$, and the initial mutual coupling matrix is chosen as an identity matrix. Figure 11.1 shows the DOA estimation of $\theta_2 = 45^\circ$ during 35 iterations using the ML and IMUSIC methods.

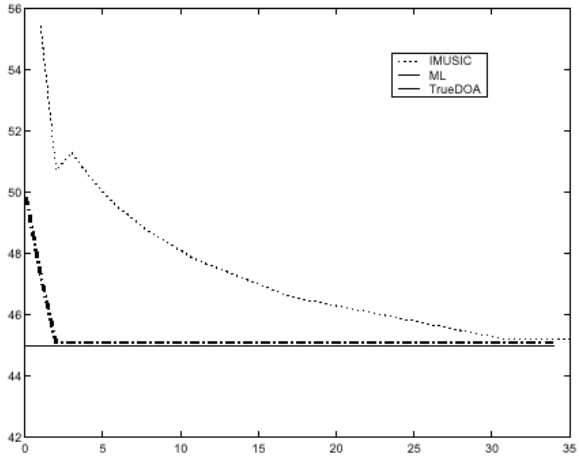

Fig.11.1 The DOA estimation of the θ =45 using the ML and IMUSIC methods versus the number of iterations using a ULA of 8 sensors when two waves are incident from 35° and 45° and 500 snapshots are taken with a SNR =30dB

In comparison with the ML method, the IMUSIC method has a slower convergence rate to the true DOA.

Figure 11.2 shows the Root Mean Square Error (RMSE) of the DOA estimation of a signal arriving from 45° using the ML and IMUSIC methods for different SNRs. In this example, an 8 sensor ULA with element spacing λ/2 is used. Two uncorrelated signals are

incident from 35˚ and 45˚ and 100 snapshots are collected. The SNR is varied from 5dB to 30dB and 30 Monte Carlo simulations are made for each simulation. From Figure 11.2 it is clear that the RMSE of the IMUSIC method is higher than that of the ML method but approaches it asymptotically for high SNRs.

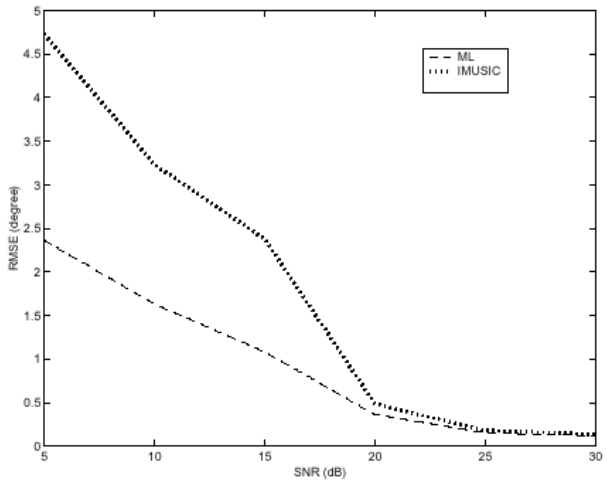

Fig.11.2 The RMSE of the DOA estimation of $\theta = 45^{\circ}$ .for ML and IMUSIC methods versus SNR using a ULA of 8 sensors with signals incident from 35˚ and 45˚ taking 100 snapshots. 30 Monte Carlo simulations are made.

11.2 DOA and Mutual Coupling Estimation with Unknown Frequencies.

For the DOA and mutual coupling estimation with multiple unknown frequencies the Separable Sub-space Method described in section 10.2.3 was used. A UCA with 8 sensors is used for the simulation and four equal-power narrow-band sources centered with two different signal frequencies are located at the far field. The four signals have the following frequencies and DOAs:

$S(\theta_{11}, f_1) = (30^{\circ}, 8.5\ \text{MHz})$, $S(\theta_{12}, f_1) = (60^{\circ}, 8.5\ \text{MHz})$,

$S(\theta_{21}, f_2) = (90^{\circ}, 6.5\ \text{MHz})$, $S(\theta_{22}, f_2) = (120^{\circ}, 6.5\ \text{MHz})$

Additive noise is injected with a SNR of 15 dB and 100 snapshots of array data are accumulated.

Figure 11.3 shows the frequency estimation. For each of the 2 estimated frequencies, Figure 11.4 and Figure 11.5 show the spatial spectrums of the DOA estimations with both unknown and estimated MCMs.

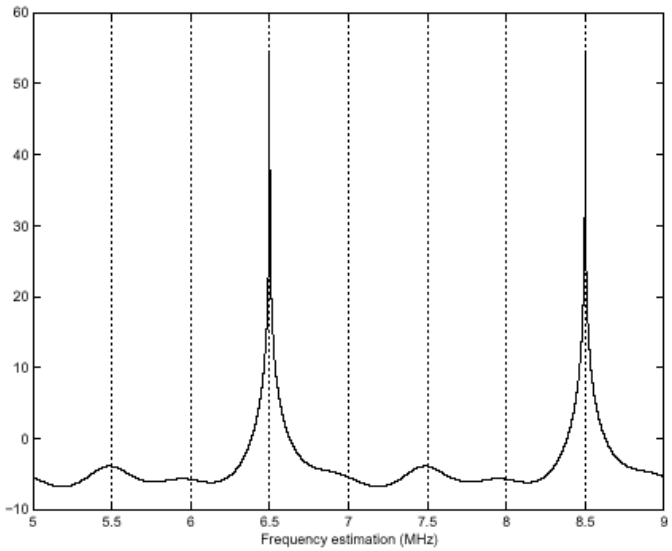

Fig.11.3 Frequency estimation by separable dimension method using a UCA of 8 sensors. Four signals with frequencies (8.5 MHz, 6.5 MHz) are incident from (30˚, 60˚) and (90˚, 120˚) with 100 snapshots. The SNR =15 dB.

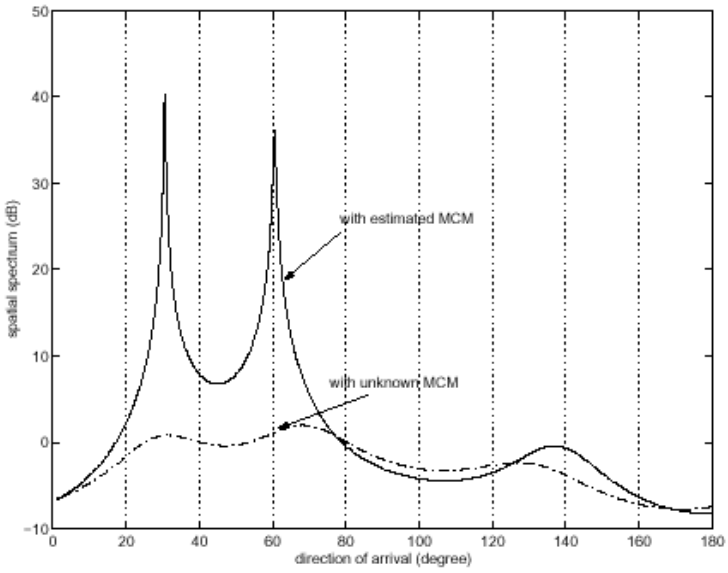

Fig.11.4 The spatial spectrum for estimated MCM and unknown MCM at the estimated frequency f_1 = 8.5 MHz using a UCA of 8 sensors. Four signals with frequencies (8.5 MHz, 6.5 MHz) are incident from (30˚, 60˚) and (90˚, 120˚) with 100 snapshots. The SNR =15 dB.

.

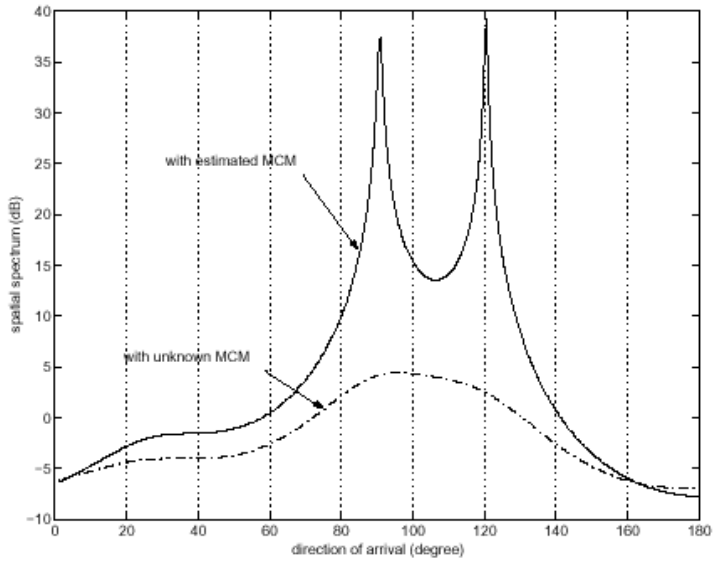

Fig.11.5 The spatial spectrum for estimated MCM and unknown MCM at the estimated frequency f_2 = 6.5 MHz using a UCA of 8 sensors. Four signals with frequencies (8.5 MHz, 6.5 MHz) are incident from (30˚, 60˚) and (90˚, 120˚) with 100 snapshots. The SNR =15 dB.

By inspecting the simulation results in Figures 11.4 and 11.5, it can be seen that the mutual coupling effect does not greatly affect the frequency estimation but severely affects the DOA estimation when using the separable dimension estimation method.

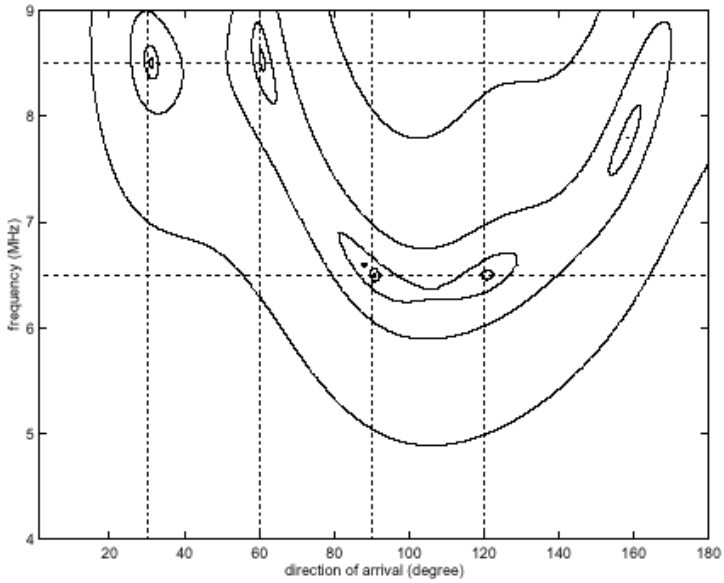

Fig.11.6 The contours of the 2D MUSIC spectrum for DOA and frequency with compensated MCM where the dotted lines represent the true DOA and frequency pairs.

Compensated with the estimated MCM, the separable dimension estimation method can estimate DOAs that are very close to the true DOAs. Figure 11.6 shows the contours of the

2D MUSIC spectrum for DOA and frequency with compensated MCM. The dotted lines indicate the true DOA/frequency pairs.

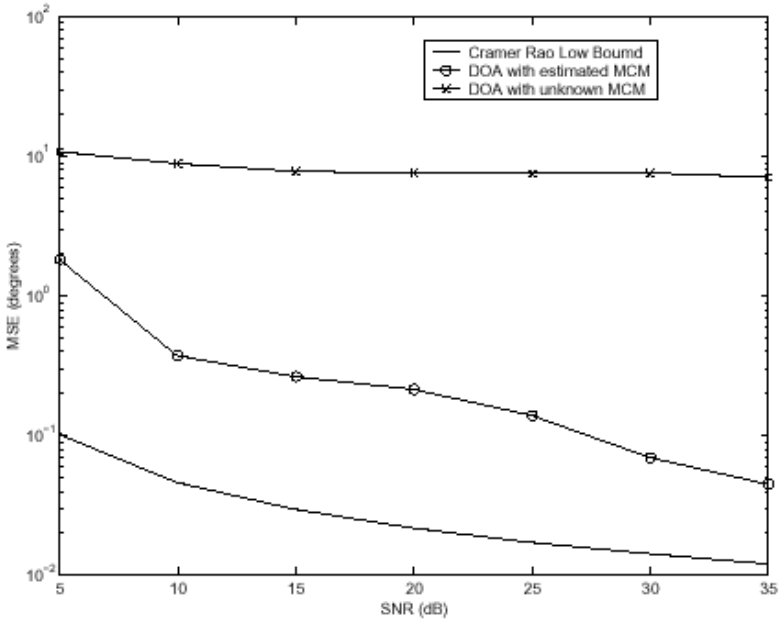

Fig.11.7 The MSE of DOA estimation of θ =30˚ using separable dimension method versus SNR using a UCA of 8 sensors and 30 Monte Carlo simulations. Four signals with frequencies (8.5 MHz, 6.5 MHz) are incident from (30˚, 60˚) and (90˚, 120˚) with 100 snapshots.

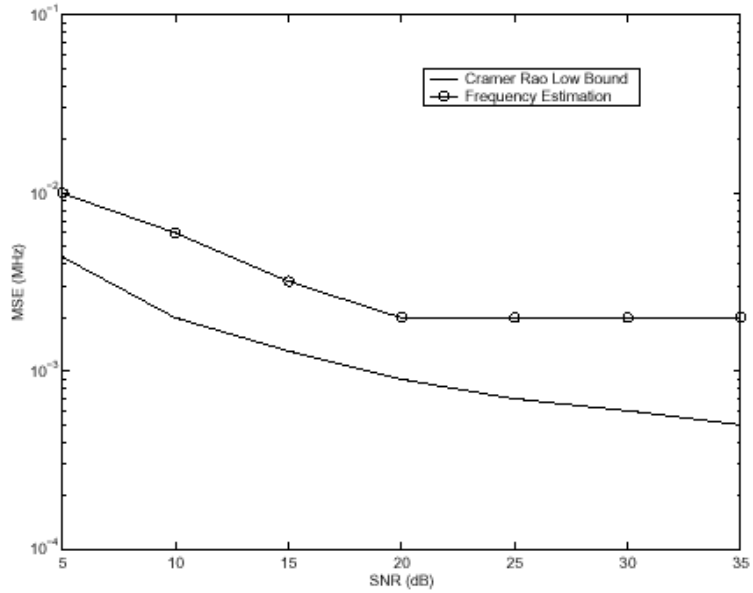

Fig.11.8 The MSE of DOA estimation of f = 8.5 MHz using separable dimension method versus SNR using a UCA of 8 sensors and 30 Monte Carlo simulations. Four signals with frequencies (8.5 MHz, 6.5 MHz) are incident from (30˚, 60˚) and (90˚, 120˚) with 100 snapshots.

Figures 11.7 and 11.8 illustrate the mean square error (MSE) of the estimated DOA and frequency, DOA =30˚ and f = 8.5 MHz, and also compare them to their theoretical lower

bound. In this example, the array and source scenarios are the same as the above example except that 150 snapshots are taken. The SNR is varied from 5 dB to 35 dB and 30 Monte Carlo simulations are made for each test.

11.3 Array Sensor Gain/Phase Error Calibration.

To simulate the simultaneous estimation of frequency, DOA and sensor gain/phase error the Alternating Iterative method of section 10.2.4 and the Global Optimisation using Simulated Annealing of section 10.2.5 were considered. For both simulations a UCA of 8 omnidirectional sensors is used.

11.3.1 Alternating Iterative Method

In this example four equal-power narrow-band sources are located in the far field of the array with the frequencies and directions:

$S(\theta_{11}, f_1) = (30^\circ, 7.5\ \text{MHz})$, $S(\theta_{12}, f_1) = (58^\circ, 7.5\ \text{MHz})$,

$S(\theta_{21}, f_2) = (85^\circ, 5.5\ \text{MHz})$, $S(\theta_{22}, f_2) = (115^\circ, 5.5\ \text{MHz})$

The SNR was set at 20 dB and 100 data samples were accumulated.

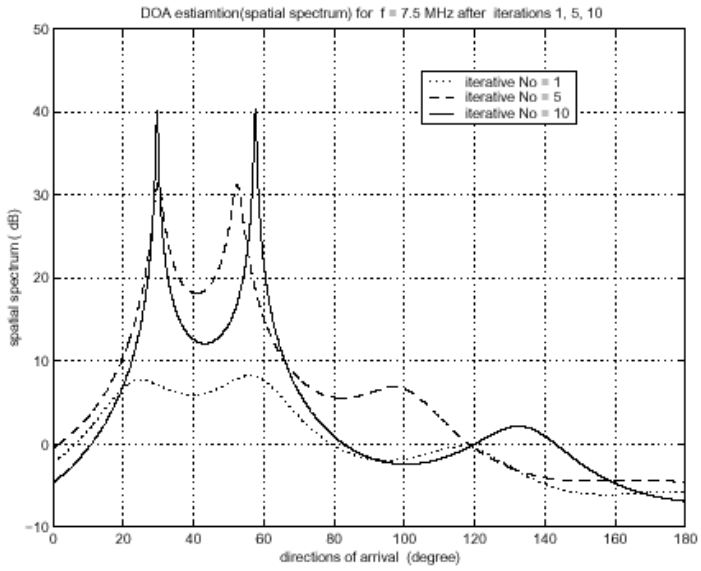

Fig.11.9 MUSIC spectrum for the Alternating Iterative method after iterations 1,6,and 10 using a UCA of 8 sensors with two signals with frequency f_1 =7 .5 MHz incident from 30˚ and 58˚. 100 snapshots with SNR =20 dB

Figures 11.9 and 11.10 show the MUSIC spectrums after iterations 1, 6 and 10 for the different estimated frequencies, f = [7.5, 5.5] MHz, respectively. It is clear from the results that after 10 iterations, the array sensor gain/phase errors have been corrected and the estimated DOAs are close to the true DOAs.

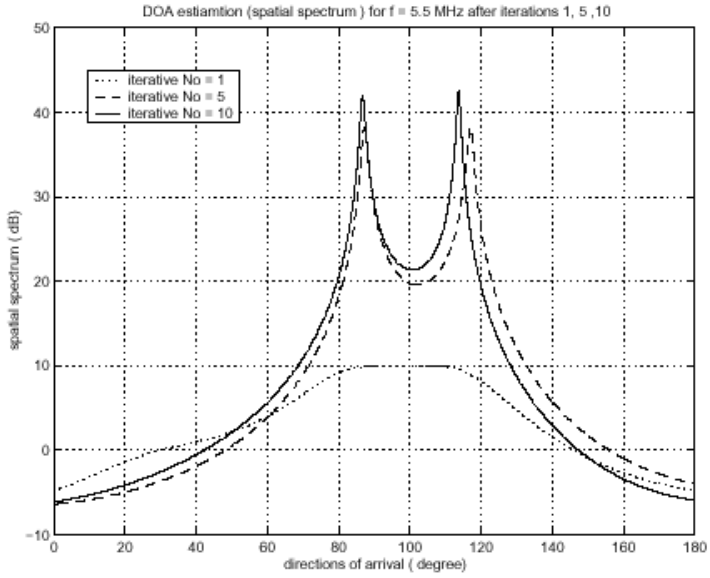

Fig.11.10 MUSIC spectrum for the Alternating Iterative method after iterations 1,6,and 10 using a UCA of 8 sensors with two signals with frequency f_2 =5 .5 MHz incident from 85˚ and 115˚. 100 snapshots with SNR =20 dB

11.3.2 Simulated Annealing Method.

Using the same array structure as the previous example, this uses a Simulated Annealing algorithm to estimate the frequency and DOA of four signals in the presence of sensor gain/phase errors. Four equal-power narrow-band sources are located in the far field of the array with the frequencies and directions:

$S(\theta_{11}, f_1) = (15^\circ, 5.5\ \text{MHz})$, $S(\theta_{12}, f_1) = (120^\circ, 5.5\ \text{MHz})$,

$S(\theta_{21}, f_2) = (150^\circ, 7.5\ \text{MHz})$, $S(\theta_{22}, f_2) = (250^\circ, 7.5\ \text{MHz})$

The SNR = 10 dB and 100 samples are accumulated. Since the annealing schedule $(T_0, n_0) \ldots (T_f, n_f)$ is a critically important element in the simulated annealing algorithm, the annealing schedule should be selected carefully to guarantee that the cost function converges to

the global optimum. Note that for different optimization problems, the annealing schedule selection will be different. The annealing schedule consists of:

Initial temperature T_0: A value T_0 should is chosen that enables the system to climb out of any local minimum.

Equilibrium condition n_i: The equilibrium condition is met when a certain number of inner circulations are accepted at that temperature.

Temperature decrease T_{i+1}: When each equilibrium state is reached, the temperature will be decreased by a constant value.

Stop criteria T_f: A certain number of outer circulations. Also, a pre-determined threshold may select it; when the cost function at the end of 2 consecutive accepted values is less than this number, the outer circulation will stop and the cost function is assumed to have reached its minimum.

Figures 11.11 and 11.12 show the results of the DOA and frequency estimations using the simulated annealing method. As can be seen, with random searching in DOA and frequency space by the simulated annealing algorithm, the curves finally converge to the corresponding DOAs and frequencies and the DOAs and frequencies are estimated simultaneously. 8000 annealing iterations are shown in the graphs. Figure 11.13 shows the cost function for the simulated annealing method where the cost function curve moves to the minimum from local stationary points. This allows the algorithm to proceed and to find a globally optimal solution.

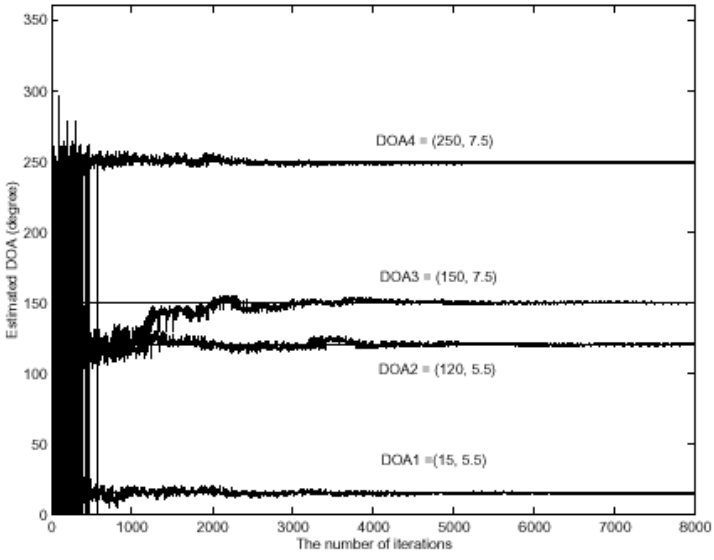

Fig.11.11 DOA estimation using simulated annealing A UCA of 8 sensors is used. 4 signals with frequencies, f_1 = 7.5 MHz and f_2 = 5.5 MHz are incident from (150˚, 250˚) and (15˚, 120˚). 100 snapshots with SNR =10dB.

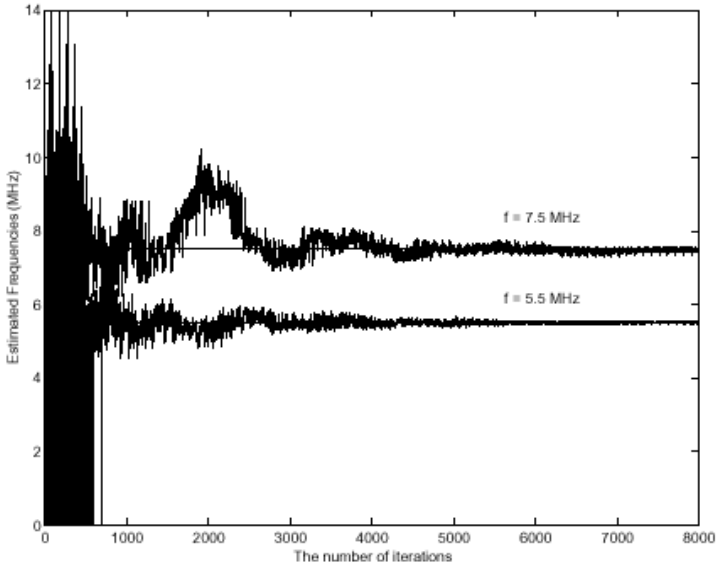

Fig.11.12 Frequency estimation using simulated annealing A UCA of 8 sensors is used. 4 signals with frequencies, f_1 = 7.5 MHz and f_2 = 5.5 MHz are incident from (150˚, 250˚) and (15˚, 120˚). 100 snapshots with SNR =10dB.

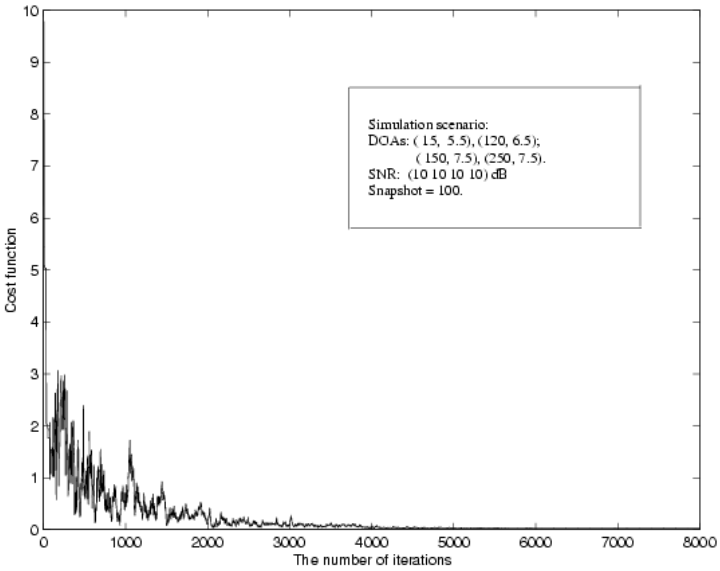

Fig.11.13 The cost function for the simulated annealing method

12. Conclusions.

12.1 Introduction.

This report is the final report of a project undertaken by the University of Limerick on behalf of the Air Force Research Laboratory (AFRL/IFGA, Rome, NY) through the European Office of Aerospace Research and Development. The main objective of the project is to investigate the possibility of using the known characteristics of GPS signals to calibrate smart antenna arrays 'on-the-fly' and thus reduce the time taken to acquire and characterise other unknown signals, especially in hostile environments. This necessitates the development of improved robust, stable and accurate estimation algorithms to process the data sampled from the sensors of an antenna array. In practice, it may be advantageous to utilise different algorithms to handle different parts of the problem.

12.2 Antenna array model and systemic errors.

In section 7 it was shown that, for an ideal antenna array, the azimuth and elevation of an unknown signal of known frequency can be calculated from the measured time delays at each sensor by reference to the ideal antenna manifold; which is itself a function of the individual sensor response and the array geometry. In practice, however, the array manifold is distorted by gain and phase errors between the sensors and their associated circuitry and mutual coupling between array elements. The gain and phase errors of the sensors are measured with respect to a reference sensor and are independent of each other; they can be described as a diagonal matrix. The effects of mutual coupling are more complex as they are dependent on the position of the sensor within the array. The effects are best described using a matrix, the Mutual Coupling Matrix (MCM), which in the usual case of symmetric arrays has a symmetric structure; for a ULA the MCM is a banded Toeplitz matrix and for a UCA it is a circulant matrix.

In particular, these errors are frequency dependent and thus severely degrade the accuracy of spatial or spatio-temporal parameter estimations when handling multiple signals with different frequencies. In this study, therefore, much effort has been put into investigating and proposing methods of estimating the gain/phase and mutual coupling errors in the situation of both known and unknown signal frequencies.

12.3 Parameter estimation methods.

For the case of signals with known frequency (as would be the case when using GPS signals) a Maximum Likelihood method (section 10.2.1) and an Iterative MUSIC method (which is a Subspace method) (section 10.2.2) were considered for the estimation of directions of arrival (DOAs) and the MCM simultaneously. Analysis of the effects of model errors and sensitivity analysis (section 9) appeared to show that the Subspace method would be more accurate. However, when simulations were run, the ML method showed a faster convergence to the actual value (section 11.1) and a lower RMSE.

For the case of multiple unknown frequency signals a Separable Dimension Subspace-based method was considered (section 10.2.3) to simultaneously estimate the signal frequencies and DOAs as well as the mutual coupling parameters. With separable dimension processing the spatial and temporal estimation problems are separated; the signal frequencies are first estimated using a subspace method and then the DOAs and MCM are estimated at each of the estimated frequencies. In this way the computational complexity is relatively low and the performance is satisfactory. Two separable subspace algorithms were developed to demonstrate the power of this approach – an Alternating Iterative method and a Global Optimisation method based on Simulated Annealing. This estimation procedure is a non-linear, multi-dimensional optimisation problem and whether or not the algorithm can converge to a global optimum depends on the choice of initial values. When simulations were run (section 11.3), both algorithms were shown to be capable of accurate frequency and DOA estimation with effective correction of systematic errors. The Global Optimisation method is far more computationally intensive as well as being sensitive to the initial annealing parameters; however, it does have the advantage of ensuring a high probability of convergence to a global optimum whereas this cannot be guaranteed using the Alternating Iterative method.

12.4 The use of GPS signals to estimate the MCM and gain/phase errors.

Signals from GPS satellites are ideal for calibrating an antenna array because they are of the same known frequency and, once the position and attitude of the array is known, the DOA of each signal is known accurately and independent of array parameters. This would enable an ML algorithm, such as that developed in section 10.2.1, to rapidly estimate the MCM and gain/phase errors; either as separate matrices or as an actual array manifold. It might be advantageous to carry out this calibration at both L1 and L2 so as to obtain some information on the frequency dependence of the error matrices.

Once we have obtained accurate MCM and gain/phase error matrices, they may be used, with rough frequency correction if available, as initial conditions for using a separable dimension algorithm (such as derived in sections 10.2.4 or 10.2.5) to estimate the frequency and DOA of unknown signals. Simulations in section 11 have shown that the speed of convergence and accuracy of these estimation methods is very dependent on the initial conditions. The use of these improved initial conditions should, therefore, speed up the estimation of the unknown parameters and increase the chance of attaining a global optimum. This may enable the faster Alternating Iterative method to be used instead of the alternative Global Optimisation using Simulated Annealing. Alternatively it may lead to faster convergence using Simulated Annealing; further investigation is necessary to evaluate the advantages of more accurate initial conditions.

We have shown that GPS signals may be used to calibrate an antenna array by estimating the MCM and gain/phase error matrix. This would provide improved initial conditions for algorithms used to estimate the frequency and DOA of unknown signals, thus ensuring faster and more accurate estimations.

13. Bibliography.

[1] H. Krim and M. Viberg, Two Decades of Array Signal Processing Research: The Parametric Approach, *IEEE Signal Processing Magazine*, 13(4): 67 - 94, July 1996.

[2] G. V. Tsoulos, Smart Antennas for Mobile Communications Systems; benefits and Challenges, *IEE Electronics and Communication Engineering Journal*, 84 – 94, April 1994.

[3] M. S. Bartlet, Smoothing Periodograms from Time Series with Continuous Spectra, *Nature*, Vol. 161:686 - 687, 1948.

[4] J. Capon, High-resolution Frequency-wavenumber Spectrum Analysis, *Proc. of IEEE*, 57(8): 1408 - 1418, August 1969.

[5] R. O. Schmidt, Multiple Emitter Location and Signal Parameter Estimation, *IEEE Trans. on Antenna and Propagation*, 34(3): 276 - 280, March 1986.

[6] M. Viberg and B. Ottersten, Sensor Array Processing Based on Subspace Fitting, *IEEE Trans. on Signal Processing*, 39(5): 1110 - 1121, May 1991.

[7] R. Roy and T. Kaliath, ESPRIT - Estimation of Signal Parameters via Rotational Invariance Techniques, *IEEE Trans. on Acoustic, Speech and Signal Processing*, 37(7):984 - 995, 1989.

[8] R. A. Fisher, On an Absolute Criterion for Fitting Frequency Curves, *Messenger of Mathematics*, Vol. 41: 155 - 160, 1912.

[9] B. Friedlander and A. J. Weiss, Direction Finding in the Presence of Mutual Coupling, *IEEE Trans. on Antennas and Propagation*, 39(3): 273 -284, March 1991

[10] J. Mao, B. Champagne, M. O'Droma and K. Kwiat, Separable Dimension Subspace Method for the Joint Signal Frequencies, DOAs and Sensor Mutual Coupling Estimation,

[11] H. Akaike, Fitting Autoregressive Models for Prediction, *Ann. Inst. Statist. Math.*, Vol. 21, pp.243 - 247, 1969

[12] P. Stoica and R. Moses, Introduction to Spectral Analysis, Prentice Hall, 1997

[13] E. Aartts and J. Korst, *Simulated Annealing and Boltzmann Machines*, John Wiley & Sons, 1990.

[14] S. Geman and G. Geman, Stochastic Relaxation, Gibbs Distribution, and Bayesian Restoration of Image, *IEEE Trans. on PAMI*, Vol.6: 721 - 741, 1984.

[15] R. Ahmed and B. L. Evans, Optimization of Signal Processing Algorithms, *Proc. of IEEE* , pp. 1401 - 1406, 1997.

[16] C. A. Balanis, Antenna Theory: Analysis and Design, John Wiley & Sons, Inc., NY 1982.

[17] G. C. Brown, J. H. McClellan and E. J. Holder, Eigenstructure Approach for Array processing and Calibration with General Phase and Gain Perturbations, *Proc. of IEEE ICASSP'91*, pp. 1365 - 1368, 1991.

[18] S. Chen, R. H. Istepanian, and B. L. Luk, Signal Processing Applications Using Adaptive Simulated Annealing, *Proc. of IEEE* , pp. 842 - 849, 1999.

[19] Y. Chen and C. Chen, Direction-of-arrival and Frequency Estimations for Narrowband Sources Using Two Single Rotation Invariance Algorithms with the Marked Subspace, *Radar and Signal Processing, IEE Proceedings - F*, 139 (4) : 297 -300, August 1992.

[20] M. P. Clark, and L. L. Scharf, Two-dimensional Modal Analysis Based on Maximum Likelihood, *IEEE Trans. on Signal Processing*, 42(6): 1443 - 1452, June 1994.

[21] H. Cramer, Mathematical Methods of Statistics, Princeton University Press, 1946.

[22] A. D. Craig, C. K. Leong and A. T. Wishar, Digital Signal Processing in Communications Satellite Payloads, *Electronics and Communications Engineering Journal*, pp.107 - 114, June 1992.

[23] R. S. Elliot, Antenna Theory and Design, Prentice-Hall, Englewood Cliffs, NJ, 1983.

[24] Emile Aartts and Jan Korst, *Simulated Annealing and Boltzmann Machines*, John Wiley \& Sons, 1990.

[25] R. B. Ertel, P. Cardieri, K. W. Sowerby, T. S. Rappaport and J. H. Reed, Overview of Spatial Channel Models for Antenna Array Communication Systems, *IEEE Personal Communications*, pp.10 - 22, February 1998.

[26] B. Friedlander, A Sensitivity Analysis of the MUSIC Algorithm, *IEEE Trans. on Acoustics, Speech, and Signal Processing*, 38(10), October 1990.

[27] A. J. Weiss and B. Friedlander, Eigenstrecture Methods for Direction Finding with Sensor Gain and Phase Uncertainties, *Circuits, Systems and Signal Processing*, Vol. 9, No. 3, pp.272 - 300, 1990.

[28] E. M. Friel and K. M. Pasala, Wideband Bearing Estimation with Compensation for Mutual Coupling Effects, *Proc. of IEEE Antenna and Propagation Symposium (AP-S/URSI'94)* , Vol. 3, pp.1556 - 1559, 1994.

[29] S. Geman and G. Geman, Stochastic Relaxation, Gibbs Distribution, and Bayesian Restoration of Image, I*EEE Trans. on PAMI*, Vol.6: 721 - 741, 1984.

[30] I. J. Gupta and A. K. Ksienski, Effect of Mutual Coupling on the Performance of Adaptive Arrays, *IEEE Trans. on Antennas and Propagation*, 31(5): 785-791, September 1983.

[31] M. H. Hayes, *Statistical Digital Signal Processing and Modeling*, John Wiley and Sons, Inc.

[32] S. Haykin, *Advances in Spectrum Analysis and Array Processing*, Vol. 2, Prentice-Hall, 1991.

[33] M. Hamid and R. Mamid, Equivalent Circuit of Dipole Antenna of Arbitrary Length, *IEEE Trans. on Antennas and Propagation*, 45(11): 1695 - 1696, November 1997.

[34] A. S. Householder, *The Theory of Matrices in Numerical Analysis*, NEW York, 1975.

[35] D. H. Johnson and D. E. Dudgen, *Array Signal Processing-Concepts and Techniques*, Prentice-Hall, 1993.

[36] S. Kirkpatric, C. D. Gellat and M. Vecchi, Optimization by Simulated Annealing, *Science*,Vol. 220, pp.671 - 680, 1983

[36] A. Leshem and M. Wax, Array calibration in the presence of multipath, *IEEE Trans. on Signal Processing*, 48(1): 53 - 59, Jan. 2000.

[37] J. T. -H. Lo and S. L. Marple, Observability Conditions for Multiple Signal Direction Finding and Array Sensor Localization, *IEEE Trans. on Signal Processing*, Vol.40: 2641 - 2650, 1992.

[38] S. Lundgren, A Study of Mutual Coupling Effects on the Direction Finding Performance of ESPRIT with a Linear Microstrip Patch Array Using the Method of Moments, *IEEE AP-S Symposium*, pp.1372 - 1375, Baltimore, USA, July 1996.

[39] D. G. Manolakis, V. K. Ingle, and S. M. Kogon, *Statistical and Adaptive Signal Processing*, McGraw-Hill , 2000.

[40] J. Mao and M. Viberg, Joint Estimation for Frequencies, Bearings and Array Model Errors by Using Simulated Annealing , *IASTED Conference on Modelling and Simulation (MS'98)*, Pittsburgh, USA, May 1998.

[41] B. C. Ng and C. M. S. See, Sensor-Array Calibration Using a Maximum-Likelihood Approach , *IEEE Trans. on Antennas and Propagation*, 44(6): 827 - 835, June 1996.

[42] B. Ottersten, M. Viberg, P. Stoica, and A. Nehorai, Exact and large Sample ML Techniques for Parameter Estimation and Detection in Array Processing, *Radar Array Processing*}, pp.99 - 151, (edited by Haykin, Litiva, and Shepherd), Springer-Verlag, Berlin, 1993.

[43] K. M. Pasala and E. M. Friel, Mutual Coupling Effects and Their Reduction in Wideband Direction of Arrival Estimation, *IEEE Trans. on Aerospace and Electronic Systems*}, 30(4): 1116 - 1122, October 1994.

[44] A. J. Pauraj and T. Kailath, Direction of Arrival Estimation by Eigenstructure Methods with Unknown Sensor Gain and Phase, *Proc. of ICASSP-85*: 17.7.1 - 17.7.3, 1985.

[45] A. J. Paulraj, R. O. Roy, and T. Kaliath, A Subspace Rotation Approach to Signal Parameter Estimation, *Proc. of IEEE*, 74(7): 1044 - 1045, 1986.

[46] D. T. Pham and D. Karaboga, *Intelligent Optimization Techniques*, Springer-Verlag, 2000.

[47] J. Pierre and M. Kaveh, Experimental Performance of Calibration and Direction-Finding Algorithms, *IEEE ICASSP'91*, Vol.2, pp.1365 - 1368, Toronto, Canada, May 1991.

[48] B. A. Pontano, Satellite Communications: Services, Systems and Technologies, *IEEE MTT-S Digest*, pp.1 - 4, 1998.

[49] K. C. Sharman, Maximum Likelihood Parameter Estimation by Simulated Annealing, *Proc. of ICASSP-88*, pp.2741 - 2744, 1988.

[50] I. S. D. Solomon, Y. I. Abramovich, D. A. Gray, and S. J. Anderson, Performance of OTH Radar Array Calibration, *IEEE ICASSP'98*, Vol.4, pp.2025 - 2028, Seattle, USA, May 1998.

[51] I. S. D. Solomon, D. A. Gray, Y. I. Abramovich, and S. J. Anderson, Over-the-horizon Radar Array Calibration Using Echoes from Ionized Meteor Trails, *IEE Proc. -Radar, Sonar Navig.*, Vol.145, No.3, pp.173 - 180, June 1998.

[52] Peter Stoica and Arye Nehorai, MUSIC, Maximum Likelihood, and Cramer-Rao Bound, *IEEE Trans. on Acoustics, Speech and Signal Processing*, 37(5): 720 -741, May 1989.

[53] T. Svantesson, The Effects of Mutual Coupling on the Direction Finding Accuracy of a Linear Array of Thin Dipoles of Finite Length, Technical report R007/1998, Department of Signals and Systems, Chalmers University of Technology, Goteborg, Sweden, August 1998.

[54] A. Swindlehurst and T. Kaliath, A Performance Analysis of Subspace-based Methods in the Presence of Model Errors - Part I: The Music Algorithm, *IEEE Trans. on Signal Processing*, 40(7): 1758 - 1774, July 1992.

[54] A. Swindlehurst and T. Kaliath, A Performance Analysis of Subspace-based Methods in the Presence of Model Errors - Part II: Multidimensional Algorithms, *IEEE Trans. on Signal Processing*, 41(9): 2882 -2890, September 1993.

[55] M. Viberg and A. L. Swindlehurst, A Bayesian Approach to Auto-Calibration for Parametric Array Signal Processing, *IEEE Trans. on Signal Processing*, 42(12): 3495 - 3506, December 1994.

[56] M. Wax and I. Ziskind, Detection of the Number of Coherent Signals by the MDL Principle , *IEEE Trans. on Acoustics, Speech and Signal Processing*, 37(8): pp.1190 - 1196, Aug. 1989.

[57] S. R. White, Concepts of Scale in Simulated Annealing, *Proc. of IEEE Conf. Computer Design: VLSL in Computers, ICCD-84*, pp.646 - 651, 1984

[58] H. Yuan, K. Hirasawa, and Y. Zhang, The Mutual Coupling and Diffraction effects on the Performance of a CMA Adaptive Array, *IEEE Vehicular Technology*, 47(3): 728 - 736, August 1998.

[59] M. Zhang and Z. Zhu, A Method for direction Finding under Sensor Gain and Phase Uncertainties, *IEEE Trans. on Antennas and Propagation*, vol. 43, pp. 880 - 883 , August 1995.

[60] I. Ziskind and M. Wax, Maximum Likelihood Localization of Diversely Polarized Sources by Simulated Annealing, *IEEE Trans. on Antennas and Propagation*, 38(7): 1111 - 1114, July 1990.

Appendix A

Paper published in
Proceedings of The IEEE 34th Asilomar Conference on Signals, Systems and Computers. IEEE 0-7803-6514-3/00, pp605-609.

October 29 - November 1, 2000, in Pacific Grove, California.

J. Mao, B. Champagne, M. O'Droma & K. Kwiat. Separable dimension subspace method for joint signal frequencies, DOAs and sensor mutual coupling estimation'.

Proceedings of
The IEEE 34th Asilomar Conference on Signals, Systems and Computers
October 29 - November 1, 2000, in Pacific Grove, California.

Separable Dimension Subspace Method for Joint Signal Frequencies, DOAs and Sensor Mutual Coupling Estimation

Jian Mao[1,2], Benoit Champagne[1], Mairtin O'Droma[2], and Kevin Kwiat[3]

[1]Dept. of Electrical and Computer Engineering
McGill University, Montreal, Quebec H3A 2A7, Canada
mao@tsp.ece.mcgill.ca, champagne@ece.mcgill.ca

[2]Dept.of Electronic and Computer Engineering
University of Limerick, Limerick, Ireland *
jain.mao, mairtin.odroma@ul.ie

[3]Air Force Research Lab
AFRL/IFGA, Rome, NY 13441-4505, USA
kwiatk@rl.af.mil

Abstract

To extract the frequencies and direction of arrivals (DOAs) of multiple sources from experimental data collected by a sensor array is a multiple parameter estimation problem. Some important algorithms for spatial-temporal processing have been developed in the past decades. A practical problem, not often considered, is that the different sensors in the array affect each other through mutual coupling. This effect varies with frequencies and degrades the performance of algorithms. Thus, a separable dimension subspace method to simultaneously estimate signal frequencies, direction of arrivals (DOAs) and sensor mutual coupling is proposed in this paper.

1. Introduction

The estimation of the frequencies and direction of arrivals (DOA's) of multiple signals by using an antenna array has attractive and important applications in various areas, such as radar and communication systems. In particular, for next generation mobile communication systems, due to an endless quest for increased capacity and improved quality, frequency and DOA estimation become a requirement. Many effective algorithms for simultaneously estimating the frequencies and DOA of multiple signals have been developed in the recent past [1, 3, 4]. Most of them assume that the array response is completely known. However, many factors, such as mutual coupling among the different array sensors, will alter the array response in practical applications. Particularly, in the presence of multiple sources with different frequencies, the sensor mutual coupling will vary with frequency and thus severely affect frequency and DOA estimation accuracy. In Reference [5], a joint signal frequencies, DOAs and array model errors estimation algorithm was proposed. Due to simulated annealing process employed, the proposed algorithm has high computation cost. In this paper, a separable dimension subspace method to simultaneously estimate signal frequencies, DOAs and mutual coupling parameters of antenna array is presented. With separable dimension processing, a spatial and temporal estimation problem is separated. i.e, the frequencies are first estimated by using a subspace method and then the DOAs and mutual coupling parameters are estimated for the each estimated frequency. In this way, the computational complexity of the proposed method is relatively small.

2. Problem Formulation

Consider an array composed of M sensors and each sensor output being fed to a tap-delay-line with m taps. The delay between adjacent taps is t_0. Specially, let $\mathbf{X}_l(t)(l = 1, 2, \cdots, M)$ denotes the output of the l-th sensor at time t, and let $\mathbf{X}_l(t) = [x_l(t), \cdots, x_l(t-(m-1)t_0)]^T$. Assume

*Thanks to American Air Force Research Lab for their funding the research work

0-7803-6514-3/00/$10.00©2000 IEEE

PROCEEDINGS OF
THE IEEE 34TH ASILOMAR CONFERENCE ON SIGNALS, SYSTEMS AND COMPUTERS
OCTOBER 29 - NOVEMBER 1, 2000, IN PACIFIC GROVE, CALIFORNIA.

that p narrow-band sources with different frequencies and directions impinge on the array and the coming signals can be divided into D groups according to their wavelength, i.e,

$$p = \sum_{k=1}^{D} p_k \qquad (D \le p) \tag{1}$$

where p_k is the number of signals, from different directions, in the $k-th$ group, which wavelength is λ_k $(k = 1, 2, \cdots, D)$.

The l-th sensor $(l = 1, 2, \cdots, M)$ output vector may be defined as:

$$\begin{aligned} &\mathbf{X}_l(t) \\ &= \sum_{k=1}^{D}\sum_{i=1}^{M}(C_{l,i}(\omega_k)\mathbf{a}(\omega_k)\mathbf{b}_i(\theta_k))\mathbf{S}_k(t) + \mathbf{N}_l(t); \\ &\qquad (k = 1, 2, \cdots, D, i = 1, 2, \cdots, M) \end{aligned} \tag{2}$$

where
$\mathbf{b}_i(\theta_k) = [\exp(-j\omega_k\tau_i(\theta_{k,1}))\cdots\exp(-j\omega_k\tau_i(\theta_{k,p_k}))]$ is a $1 \times p_k$ spatial steering vector;
$\mathbf{a}(\omega_k) = [1 \quad \exp(-j\omega_k t_0)\cdots\exp(-j\omega_k(m-1)t_0)]^T$ is an $m \times 1$ temporal steering vector; $C_{l,i}(\omega_k)$ is the $(l,i)-th$ entry in the mutual coupling matrix (MCM) which represents the mutual coupling effect from other sensors;

$\mathbf{S}_k(t) = [S_{k,1}(t)\cdots S_{k,p_k}(t)]^T$ is a $p_k \times 1$ signal vector from the k-th group of narrowband sources and $\mathbf{N}_l = [N_l(t)\cdots N_l(t-(m-1)t_0)]^T$ is an $m \times 1$ additive noise vector for the l-th sensor.

Therefore, the array data model can be described as follows:

$$\begin{aligned} \mathbf{X}(t) &= \left[\mathbf{X}^T{}_1(t)\mathbf{X}^T{}_2(t)\cdots\mathbf{X}^T{}_M(t)\right]^T \\ &= \sum_{k=1}^{D}(\mathbf{C}(\omega_k)\mathbf{B}(\theta_k)) \otimes \mathbf{a}(\omega_k)\mathbf{S}_k(t) + \mathbf{N}(t) \end{aligned} \tag{3}$$

where

$$\mathbf{B}(\theta_k) = \begin{bmatrix} \mathbf{b}_1(\theta_k) \\ \vdots \\ \mathbf{b}_M(\theta_k) \end{bmatrix}$$

is a $M \times p_k$ spatial steering matrix, $\mathbf{N}(t) = \left[\mathbf{N}^T{}_1(t)\,\mathbf{N}^T{}_2(t)\cdots\mathbf{N}^T{}_M(t)\right]^T$ is $Mm \times 1$ additive white Gaussian noise, Symbol $\otimes$ denotes Kronecker product and $\mathbf{C}(\omega_k)$ $(k = 1, 2, \cdots, D)$ is $M \times M$ mutual coupling matrix. For a uniform linear array or circular array, $\mathbf{C}(\omega_k)$ is either a Toeplitz matrix or a circular matrix, respectively [6].

Based on the available samples $\{\mathbf{X}(t)\}_{t=1}^{N}$, the problem is to estimate the frequencies, DOAs and mutual coupling matrix simultaneously with subspace methods.

3 Subspace Method

Assume that the number of signals p and the number of frequency groups, D, are known.

Define

$$\mathbf{r}'_h = \frac{1}{M}\sum_{l=1}^{M} E[x_l(t-(h-1)t_0)\mathbf{X}_l^H(t)] \qquad (h = 1, 2, \cdots, D) \tag{4}$$

$$\boldsymbol{\eta}'_l = \frac{1}{m}\sum_{h=1}^{m} \mathrm{E}[y_l(t-(h-1)t_0)\mathbf{Y}^H(t-(h-1)t_0)] \qquad (l = 1, 2, \cdots, p) \tag{5}$$

where

$$\begin{aligned} &y_l(t-(h-1)t_0) = (\mathbf{X}_l(t))_h = x_l(t-(h-1)t_0), \\ &\mathbf{Y}(t-(h-1)t_0) \\ &= [y_1(t-(h-1)t_0)y_2(t-(h-1)t_0)\cdots y_M(t-(h-1)t_0)]^T \\ &= [x_1(t-(h-1)t_0)x_2(t-(h-1)t_0)\cdots x_M(t-(h-1)t_0)]^T \end{aligned}$$

and $E(\cdot)$ denotes statistical expectation.

$\{\mathbf{r}'_h\}_{h=1}^{D}$ and $\{\boldsymbol{\eta}'_l\}_{l=1}^{p}$ are frequency vector and direction vector. Their range spaces spanned by the column of these vectors which are contained or are equal to the range spaces of $\mathbf{a}(\omega)$and $\mathbf{B}(\theta)$, respectively. We have

$$\Re(\mathbf{r}'_h) \subseteq \Re(\mathbf{a}(\omega)), \quad \Re(\boldsymbol{\eta}'_l) \subseteq \Re(\mathbf{B}(\theta))$$

and

$$\aleph(\mathbf{r}'_h) \perp \Re(\mathbf{a}(\omega)), \quad \aleph(\boldsymbol{\eta}'_l) \perp \Re(\mathbf{B}(\theta))$$

where $\Re(\cdot)$ and $\aleph(\cdot)$denote the range space and null space. As is well known, the subspace methods are based on the above geometrical observations.Therefore,we may use correlation processing in spatial and temporal dimension respectively to get the estimates of $\{\mathbf{r}'_h\}_{h=1}^{D}$ and $\{\boldsymbol{\eta}'_l\}_{l=1}^{p}$ and then compute their null subspaces. Finally, the frequencies, DOAs and mutual coupling matrix can be finally estimated with subspace methods by searching corresponding spaces.

4 Separable Dimension Subspace Algorithm

Step 1. Frequency Estimation
(1) Estimate of frequency vectors $\mathbf{r}'_h$ and $\mathbf{r}_h$:

$$\hat{\mathbf{r}}'_h = \frac{1}{M}\sum_{l=1}^{M}\frac{1}{N}\sum_{t=1}^{N} x_l(t-(h-1)t_0)\mathbf{X}_l^H(t) \tag{6}$$

PROCEEDINGS OF
THE IEEE 34TH ASILOMAR CONFERENCE ON SIGNALS, SYSTEMS AND COMPUTERS
OCTOBER 29 - NOVEMBER 1, 2000, IN PACIFIC GROVE, CALIFORNIA.

$$\hat{\mathbf{r}}_h = (\hat{\mathbf{r}}'_h - \hat{\sigma}^2 \mathbf{e}_h)^H, \tag{7}$$

where

$$\mathbf{e}_h = [\underbrace{0 \cdots 0}_{(h-1)} 1 0 \cdots 0],$$
$$(h = 1, 2, \cdots, D)$$

and $\hat{\sigma}^2$ is the estimate of the noise variance.

(2) Gram-Schmidt (GS) orthogonalization and formation of temporal projection matrix $\mathbf{P}_\omega$:

From the vector $\{\hat{\mathbf{r}}_h\}_{h=1}^D$, we can get D orthogonal vectors, $\{\mathbf{q}_k\}_{k=1}^D$ via GS orthogonalization. Let $\mathbf{Q}_\omega = [\mathbf{q}_1, \mathbf{q}_2, \cdots, \mathbf{q}_D]$, then compute the temporal projection matrix $\mathbf{P}_\omega = \mathbf{I} - \mathbf{Q}_\omega \mathbf{Q}_\omega^H$, which spans the null space of $\{\mathbf{a}(\omega_k)\}_{k=1}^D$.

(3) Estimate the unknown frequencies with the temporal projection matrix $\mathbf{P}_\omega$:

The frequencies $\{\omega_k\}_{k=1}^D$ are estimated as the D largest peaks of the function $P(\omega) = (\mathbf{a}^H(\omega)\mathbf{P}_\omega \mathbf{a}(\omega))^{-1}$, searching over the frequency sector of interest.

Step 2. Direction and Mutual Coupling Estimation

(1)Estimate of direction vectors, η'_l and η_l:

$$\hat{\eta}'_l = \frac{1}{m}\sum_{h=1}^{m}\frac{1}{N}\sum_{t=1}^{N} y_l(t-(h-1)t_0)\mathbf{Y}^H(t-(h-1)t_0) \tag{8}$$

$$\hat{\eta}_l = (\hat{\eta}'_l - \hat{\sigma}^2 \mathbf{e}_l)^H, \tag{9}$$

where

$$\mathbf{e}_l = [\underbrace{0 \cdots 0}_{(l-1)} 1 0 \cdots 0]$$
$$(l = 1, 2, \cdots, p)$$

(2) Via Gram-Schmit orthogonalization of $\{\hat{\eta}_l\}_{l=1}^p$, the p orthogonal vectors, $\{\zeta_l\}_{l=1}^p$ and spatial orthogonal projection matrix $\mathbf{P}_\theta = \mathbf{I} - \mathbf{Q}_\theta \mathbf{Q}_\theta^H$ are obtained, where $\mathbf{Q}_\theta$=$[\zeta_1$ $\zeta_2 \cdots \zeta_p]$

(3) For each frequency $\{\omega_k\}_{k=1}^D$ estimated in Step 1, the directions θ_k and mutual coupling matrix $\mathbf{C}(\omega_k)$ can be estimated with following equations iteratively :

$$(\mathbf{B}^H(\theta)\mathbf{C}^H(\omega_k)\mathbf{P}_\theta \mathbf{C}(\omega_k)\mathbf{B}(\theta))^{-1}$$

$$\hat{\mathbf{C}}(\omega_k) = (\mathbf{G}(\omega_k)^{-1}\mathbf{w})(\mathbf{w}^H \mathbf{G}(\omega_k)^{-1}\mathbf{w})^{-1}$$

where $\mathbf{G}(\omega_k) = \sum_{k=1}^{p_k} \mathbf{B}(\theta_k)^H \mathbf{P}_\theta \mathbf{B}(\theta_k)$ and $\mathbf{w} = [1, 0, \cdots, 0]^T$.

5 Computer Simulations

A uniform circular array with 8 sensors is used for the simulation. Four equal-power narrow-band sources are located at the far field of the array with the center frequencies and directions: $S(\theta_{11}, f_1) = (30°, 8.5MHz)$, $S(\theta_{12}, f_1) = (60°, 8.5MHz)$, $S(\theta_{21}, f_2) = (90°, 6.5MHz)$, $S(\theta_{22}, f_2) = (120°, 6.5MHz)$. Additive noise is injected with SNR of 15 dB referenced to the signal source. 100 snapshots of array data are accumulated. Fig.1 shows the frequency estimation. For the 2 estimated frequencies, Fig.2 and Fig.3 show the spatial spectrum for the DOA estimations with unknown and estimated MCM, respectively. Fig.4 and Fig5 show the mean square error (MSE) of estimated DOA and frequency and their theoretical low bound. 30 Monte Carlo simulations are made for the $DOA = 30°$ and $f = 8.5MHz$

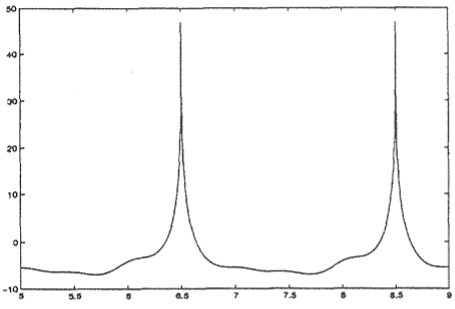

Figure 1. Frequency Estimation

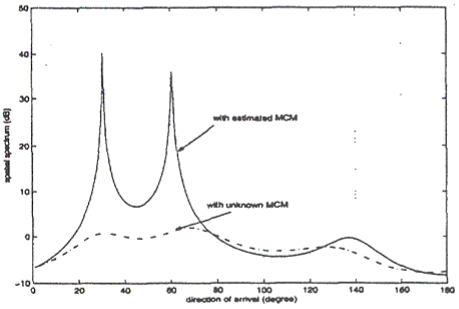

Figure 2. Spatial spectrum at the estimated frequency $f = 8.5MHz$.

6 Conclusions

In this paper a new algorithm based on separable dimension subspace method is proposed for joint estimation of signal frequencies, DOAs and the mutual coupling parameters of antenna array. The presented algorithm has been test by computer simulation studies and has been found to perform satisfactorily.

PROCEEDINGS OF
THE IEEE 34TH ASILOMAR CONFERENCE ON SIGNALS, SYSTEMS AND COMPUTERS
OCTOBER 29 - NOVEMBER 1, 2000, IN PACIFIC GROVE, CALIFORNIA.

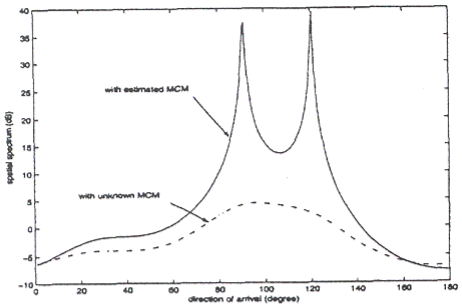

Figure 3. Spatial spectrum at the estimated frequency $f = 6.5MHz$.

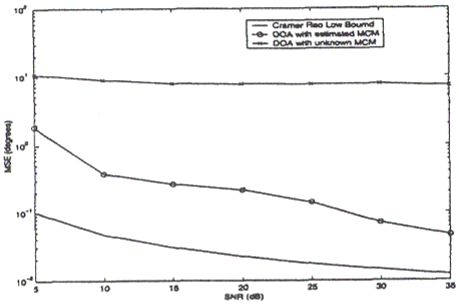

Figure 4. MSE and CRLB for the DOA estimation,$DOA = 30°$

7 Appendix: Cramer Rao Low Bound

In this appendix, we derived Cramer Rao Low Bound for the proposed separable subspace method.

The likelihood function for the data set is given by

$$L(\mathbf{X}(1), \mathbf{X}(2), \cdots, \mathbf{X}(N)/\Phi) = \prod_{j=1}^{N} \frac{1}{\pi^M |\mathbf{R}|} \exp(-\mathbf{X}(j)^H \mathbf{R}^{-1} \mathbf{X}(j)) \quad (10)$$

where $\mathbf{X}(j) = \sum_{k=1}^{D} \mathbf{C}(\omega_k)\mathbf{B}(\theta_k) \bigotimes \mathbf{a}(\omega_k)\mathbf{S}_k(j) + \mathbf{N}(j)$, $\Phi = (\theta, \omega, \mathbf{C})$, and matrix $\mathbf{R}$ is

$$\mathbf{R} = E\left[\mathbf{X}\mathbf{X}^H\right] = \sum_{k=1}^{D} \mathbf{C}(\omega_k)\mathbf{B}(\theta_k) \otimes \mathbf{a}(\omega_k)\mathbf{R}_{sk} \quad (11)$$

$$(\mathbf{C}(\omega_k)\mathbf{B}(\theta_k) \otimes \mathbf{a}(\omega_k))^H + \sigma_{nk}^2 \mathbf{I}$$

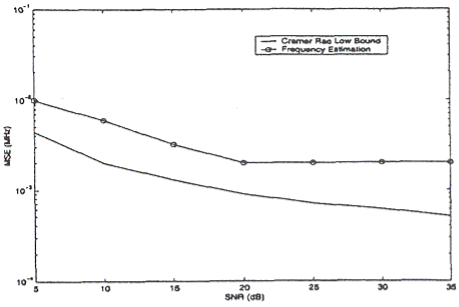

Figure 5. MSE and CRLB for the frequency estimation, $f = 8.5MHz$

Assuming all sources have signal-noise rate $P = \mathbf{R}_{sk}/\sigma_n^2$, then the Cramer Rao low bound is

$$CRLB(\Phi) = [J_{mn}]^{-1} \quad (12)$$

where the $m, n - th$ element of the Fisher information matrix are

$$J_{mn} = N \cdot tr\{\mathbf{R}^{-1} \cdot \partial\mathbf{R}/\partial\Phi_m \cdot \mathbf{R}^{-1} \cdot \partial\mathbf{R}/\partial\Phi_n\} \quad (13)$$

7.1 DOA terms

$$J_{\theta\theta} = 2N \cdot \Re(tr(\dot{\mathbf{A}}_\theta P \mathbf{A}^H \mathbf{R}^{-1} \mathbf{A} P \dot{\mathbf{A}}_\theta^H \mathbf{R}^{-1}) + tr(\dot{\mathbf{A}}_\theta P \mathbf{A}^H \mathbf{R}^{-1} \dot{\mathbf{A}}_\theta P \mathbf{A}^H \mathbf{R}^{-1})) \quad (14)$$

where $\mathbf{A} = \mathbf{C}\,\mathbf{B}(\theta) \otimes \mathbf{a}(\omega)$ and $\dot{\mathbf{A}}_\theta = \mathbf{C}\,(\partial\mathbf{B}(\theta)/\partial\theta) \otimes \mathbf{a}(\omega) = \mathbf{C}\,\dot{\mathbf{B}}(\theta) \otimes \mathbf{a}(\omega)$.

7.2 Frequency ω terms

$$J_{\omega\omega} = 2N \cdot \Re(tr(\dot{\mathbf{A}}_\omega P \mathbf{A}^H \mathbf{R}^{-1} \mathbf{A} P \dot{\mathbf{A}}_\omega^H \mathbf{R}^{-1}) + tr(\dot{\mathbf{A}}_\omega P \mathbf{A}^H \mathbf{R}^{-1} \dot{\mathbf{A}}_\omega P \mathbf{A}^H \mathbf{R}^{-1})) \quad (15)$$

where

$$\dot{\mathbf{A}}_\omega = \mathbf{C}(\partial\mathbf{B}(\theta)/(\partial\omega) \otimes \mathbf{a}(\omega) + \mathbf{C}\mathbf{B}(\theta) \otimes (\partial\mathbf{a}(\omega)/\partial\omega) = \mathbf{C}\dot{\mathbf{B}}_\omega \otimes \mathbf{a} + \mathbf{C}\,\mathbf{B} \otimes \dot{\mathbf{a}}_\omega$$

7.3 Mutual coupling terms

Suppose circulant mutual coupling matrix with only a single coupling coefficient given by

$$C_{12} = \mu e^{j\xi} \quad (16)$$

PROCEEDINGS OF
THE IEEE 34TH ASILOMAR CONFERENCE ON SIGNALS, SYSTEMS AND COMPUTERS
OCTOBER 29 - NOVEMBER 1, 2000, IN PACIFIC GROVE, CALIFORNIA.

where μ and ξ are magnitude and phase of mutual coupling coefficient. Then, we have

$$\begin{aligned} J_{\mu\mu} &= 2N \cdot \Re\,(tr\,(\dot{\mathbf{A}}_\mu P \mathbf{A}^H \mathbf{R}^{-1} \mathbf{A} P \dot{\mathbf{A}}_\mu^H \mathbf{R}^{-1}) \\ &\quad + tr\,(\dot{\mathbf{A}}_\mu P \mathbf{A}^H \mathbf{R}^{-1} \dot{\mathbf{A}}_\mu P \mathbf{A}^H \mathbf{R}^{-1})) \\ J_{\xi\xi} &= 2N \cdot \Re\,(tr\,(\dot{\mathbf{A}}_\xi P \mathbf{A}^H \mathbf{R}^{-1} \mathbf{A} P \dot{\mathbf{A}}_\xi^H \mathbf{R}^{-1}) \\ &\quad + tr\,(\dot{\mathbf{A}}_\xi P \mathbf{A}^H \mathbf{R}^{-1} \dot{\mathbf{A}}_\xi P \mathbf{A}^H \mathbf{R}^{-1})) \end{aligned} \tag{17}$$

where $\dot{\mathbf{A}}_\mu = (\partial \mathbf{C}/\partial\mu)\cdot\mathbf{B}\otimes\mathbf{a}$ and $\dot{\mathbf{A}}_\xi = (\partial \mathbf{C}/\partial\xi)\cdot\mathbf{B}\otimes\mathbf{a}$

7.4 Cross terms

The cross terms are derived as

$$J_{\theta\omega} = 2N \cdot \Re\,(tr\,(\dot{\mathbf{A}}_\theta P \mathbf{A}^H \mathbf{R}^{-1} \mathbf{A} P \dot{\mathbf{A}}_\omega^H \mathbf{R}^{-1}) + tr\,(\dot{\mathbf{A}}_\theta P \mathbf{A}^H \mathbf{R}^{-1} \dot{\mathbf{A}}_\omega P \mathbf{A}^H \mathbf{R}^{-1})) \tag{18}$$

$$J_{\theta\mu} = 2N \cdot \Re\,(tr\,(\dot{\mathbf{A}}_\theta P \mathbf{A}^H \mathbf{R}^{-1} \mathbf{A} P \dot{\mathbf{A}}_\mu^H \mathbf{R}^{-1}) + tr\,(\dot{\mathbf{A}}_\theta P \mathbf{A}^H \mathbf{R}^{-1} \dot{\mathbf{A}}_\mu P \mathbf{A}^H \mathbf{R}^{-1})) \tag{19}$$

$$J_{\theta\xi} = 2N \cdot \Re\,(tr\,(\dot{\mathbf{A}}_\theta P \mathbf{A}^H \mathbf{R}^{-1} \mathbf{A} P \dot{\mathbf{A}}_\xi^H \mathbf{R}^{-1}) + tr\,(\dot{\mathbf{A}}_\theta P \mathbf{A}^H \mathbf{R}^{-1} \dot{\mathbf{A}}_\xi P \mathbf{A}^H \mathbf{R}^{-1})) \tag{20}$$

$$J_{\omega\mu} = 2N \cdot \Re\,(tr\,(\dot{\mathbf{A}}_\omega P \mathbf{A}^H \mathbf{R}^{-1} \mathbf{A} P \dot{\mathbf{A}}_\mu^H \mathbf{R}^{-1}) + tr\,(\dot{\mathbf{A}}_\omega P \mathbf{A}^H \mathbf{R}^{-1} \dot{\mathbf{A}}_\mu P \mathbf{A}^H \mathbf{R}^{-1})) \tag{21}$$

$$J_{\omega\xi} = 2N \cdot \Re\,(tr\,(\dot{\mathbf{A}}_\omega P \mathbf{A}^H \mathbf{R}^{-1} \mathbf{A} P \dot{\mathbf{A}}_\xi^H \mathbf{R}^{-1}) + tr\,(\dot{\mathbf{A}}_\omega P \mathbf{A}^H \mathbf{R}^{-1} \dot{\mathbf{A}}_\xi P \mathbf{A}^H \mathbf{R}^{-1})) \tag{22}$$

$$J_{\mu\xi} = 2N \cdot \Re\,(tr\,(\dot{\mathbf{A}}_\mu P \mathbf{A}^H \mathbf{R}^{-1} \mathbf{A} P \dot{\mathbf{A}}_\xi^H \mathbf{R}^{-1}) + tr\,(\dot{\mathbf{A}}_\mu P \mathbf{A}^H \mathbf{R}^{-1} \dot{\mathbf{A}}_\xi P \mathbf{A}^H \mathbf{R}^{-1})) \tag{23}$$

References

[1] M. Viberg and P. Stoica, A computationally efficient method for joint direction finding and frequency estimation in colored noise. *The Thirty-Second Asilomar Conference on Signals, Systems and Computers*, pp.1547 -1551, vol.2, Nov.1998.

[2] A. N. Lemma, A.-J. van der Veen, and E. F. Deprettere, Joint angle-frequency estimation using multi-resolution ESPRIT . *IEEE International Conference on Acoustics, Speech and Signal Processing,(ASSP'98)*,1957 - 1960,vol.4, Seattle, U.S.A, May 1998.

[3] A. N. Lemma, A.-J. van der Veen, and E. F. Deprettere, Joint angle-frequency estimation for slow frequency hopping signals . *IEEE Workshop on Circuits, System and Signal Processing (CSSP'98)*, pp. 363 - 370, Mirlo, Netherlands, November 1998.

[4] J. Mao and L. Ge, A new estimation method for signal frequency and directions with array antennas. *IEEE Antenna and Propagation Sympoisum (AP-S/URSI'98)*, pp. 195 - 198, Atalanta, USA, June 1998.

[5] J. Mao and M. Viberg, Joint estimation for frequencies, bearings and array model errors by using simulated annealing . *IASTED Conference on Modelling and Simulation (MS'98)*, Pittsburg, USA, May 1998.

[6] B. Friedlander and A. J. Weiss, Direction finding in the presence of mutual coupling. *IEEE trans. on Antennas and Propagation*, 39(3): 273 -284, March 1991.

[7] T. Svantesson, Direction finding in the presence of mutual coupling. *Licenciate thesis*, Department of Signals and Systems, Chalmers Univ. of Tech., Göteborg, Sweden, March 1999.